

1

2 **Nickel in soil and water: Sources, biogeochemistry, and remediation using**
3 **biochar**

4

5 **Published in:** *Journal of Hazardous Materials*

6

7 **Citation for published version:** El-Naggar, A., Ahmed, N., Mosa, A., Niazi, N.K., Yousaf,
8 B., Sharma, A., Sarkar, B., Cai, Y., Chang, S.X., (2021) Nickel in soil and water: Sources,
9 biogeochemistry, and remediation using biochar. *Journal of Hazardous Materials*. 419:
10 126421. doi: 10.1016/j.jhazmat.2021.126421.

11

12 **Document version:** Accepted peer-reviewed version.

13

14 **Nickel in soil and water: Sources, biogeochemistry, and remediation using biochar**

15

16 Ali El-Naggar^{a,b}, Naveed Ahmed^c, Ahmed Mosa^d, Nabeel Khan Niazi^{e,f}, Balal Yousaf^g,
17 Anket Sharma^{a,h}, Binoy Sarkarⁱ, Yanjiang Cai^a, Scott X. Chang^{a,j,*}

18

19 ^a *State Key Laboratory of Subtropical Silviculture, Zhejiang A&F University, Lin'an 311300,*
20 *China*

21 ^b *Department of Soil Sciences, Faculty of Agriculture, Ain Shams University, Cairo 11241,*
22 *Egypt*

23 ^c *U.S. Pakistan Center for Advanced Studies in Water, Mehran University of Engineering*
24 *and Technology, Jamshoro, 76062, Sindh, Pakistan*

25 ^d *Soils Department, Faculty of Agriculture, Mansoura University, Mansoura 35516, Egypt*

26 ^e *Institute of Soil and Environmental Sciences, University of Agriculture Faisalabad,*
27 *Faisalabad 38040, Pakistan*

28 ^f *School of Civil Engineering and Surveying, University of Southern Queensland,*
29 *Toowoomba 4350 Queensland, Australia*

30 ^g *Department of Environmental Engineering, Middle East Technical University, Ankara*
31 *06800, Turkey*

32 ^h *Department of plant science and land Architecture, University of Maryland, college park,*
33 *USA*

34 ⁱ *Lancaster Environment Centre, Lancaster University, Lancaster, LA1 4YQ, UK*

35 ^j *Department of Renewable Resources, University of Alberta, Edmonton, Alberta, T6G 2H1,*
36 *Canada*

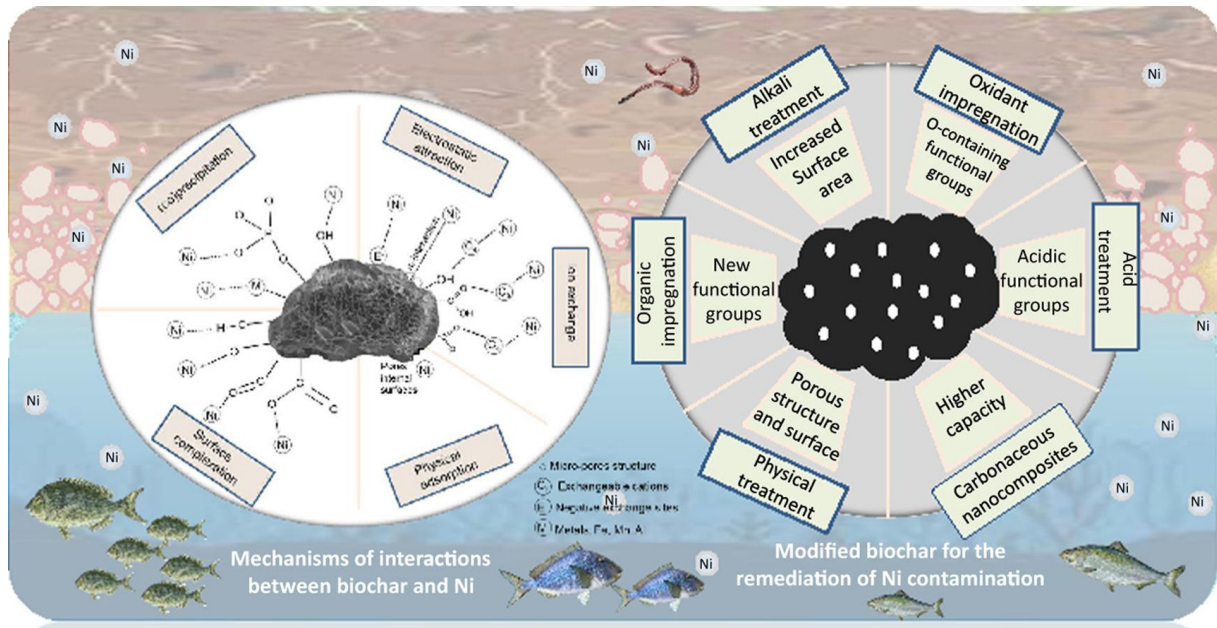
37

38 * Corresponding author: sxchang@ualberta.ca

39

40

41 Graphical abstract



42

43

44 Highlights

- 45 ➤ Ni occurrence and biogeochemistry, and remediation using biochar are reviewed.
- 46 ➤ Biochar affects redox-mediated transformations and reduces Ni availability.
- 47 ➤ Negative-charged acidic functional groups act as electron donors, enhance Ni
- 48 removal.
- 49 ➤ Competitive adsorption on binding sites on biochar may impair Ni remediation.
- 50 ➤ Biochars should be fabricated and designed for Ni remediation.

51

52 ABSTRACT

53 Nickel (Ni) is a potentially toxic element that contaminates soil and water, threatens food
54 and water security, and hinders sustainable development on a global scale. Biochar has
55 emerged as a promising novel material for remediating Ni-contaminated environments.
56 However, the potential for pristine and functionalized biochars to immobilize/adsorb Ni in
57 soil and water, and the mechanisms involved have not been systematically reviewed. Here,
58 we critically review the different dimensions of Ni contamination and remediation in soil
59 and water, including its occurrence and biogeochemical behavior under different
60 environmental conditions and ecotoxicological hazards, and its remediation using biochar.
61 Biochar is effective in immobilizing Ni in soil and water via ion exchange, electrostatic
62 attraction, surface complexation, (co)precipitation, physical adsorption, and reduction due to
63 the biogeochemistry of Ni and the interaction of Ni with surface functional groups and
64 organic/inorganic compounds contained in biochar. The efficiency for Ni removal is
65 consistently greater with functionalized than pristine biochars. Physical (e.g., ball milling)
66 and chemical (e.g., alkali/acidic treatment) activation achieve higher surface area, porosity,
67 and active surface groups on biochar that enhance Ni immobilization. This review highlights
68 possible risks and challenges of biochar application in Ni remediation, suggests future
69 research directions, and discusses implications for environmental agencies and decision-
70 makers.

71

72 *Keywords:* Biowaste; Charcoal; Immobilization; Review; Soil contamination; Sorption;
73 Toxic trace element; Wastewater

74 **1. Introduction**

75 Nickel (Ni) is a potentially toxic element that is commonly found in soil and water
76 systems. It is a transition metal with a high density (8.9 g cm^{-3}), melting point ($1455 \text{ }^\circ\text{C}$),
77 and boiling point ($2730 \text{ }^\circ\text{C}$) (Gonnelli and Renella, 2013; Tsadilas and Rinklebe, 2018).
78 Nickel has an average atomic weight of 58.69, belongs to Group X of the periodic table and
79 the iron family, along with Fe and Co (Kabata-Pendias, 2011). Nickel has four oxidation
80 states (+1, +2, +3 and +4), while its main oxidation state is +2. The Ni(II) is readily
81 available and more toxic in cationic form than its complexes (Albanese et al., 2015; Parades-
82 Aguilar et al., 2021). Nickel is widely released into soil and water systems from various
83 anthropogenic and natural sources. For example, Ni can be discharged into the environment
84 from Ni alloy industries, pigment manufacturing processes, tannery industry wastewater,
85 and mafic and ultramafic rocks and their derived soils as a result of weathering and
86 pedogenesis (Albanese et al., 2015; Babaahmadifooladi et al., 2020; Panagopoulos et al.,
87 2015). Improper disposal of industrial wastes and aerial deposition of contaminants can lead
88 to elevated levels of Ni in soil and water systems. Generally, the levels of Ni is $5\text{-}40 \text{ ng m}^{-3}$
89 in the air, $3\text{-}1000 \text{ mg kg}^{-1}$ in agricultural soils, and less than $2 \text{ } \mu\text{g L}^{-1}$ in fresh water and
90 oceans (WHO, 2000). Nickel contamination can be transferred directly from air and soil to
91 surface water bodies through deposition and runoff from soil, or indirectly to groundwater
92 via leaching (Tsadilas and Rinklebe, 2018). The pollution of this metal is increasingly
93 becoming a concern, particularly in developing countries, due to its non-degradability in the
94 environment (Panagopoulos et al., 2015; Poznanović Spahić et al., 2019).

95 The presence of excessive amounts of Ni over permissible limit in soil (35 mg kg^{-1})
96 and water (0.02 mg L^{-1}) causes toxicity to all living organisms (Antoniadis et al., 2017;
97 Hussain et al., 2017; WHO, 1996). Even though Ni is an essential micronutrient for plants
98 with concentrations $<10 \text{ mg kg}^{-1}$ of plant biomass (Sugawara and Nikaido, 2014) and in the
99 biochemistry of human microbiota at low consumption rate of $5 \text{ } \mu\text{g Ni kg}^{-1} \text{ body weight day}^{-1}$

100 ¹ (Russell et al., 2001), a high rate of intake of Ni may cause serious harm to human health,
101 such as causing allergy, cancer and reduced lung function (Zambelli et al., 2016). Therefore,
102 high concentrations of Ni in drinking water and the soil, or the entry of Ni into the food
103 chain via plant uptake poses a significant health threat for humans and animals, and
104 threatens the ecological sustainability of the global system (Rinklebe et al., 2019; Shaheen et
105 al., 2020).

106 Several techniques, including soil washing (Zou et al., 2019), adsorption (Cheng et
107 al., 2019; Fiyadh et al., 2019), reduction (Di Palma et al., 2015), membrane process
108 (Samantaray et al., 2019), electrokinetic remediation (Wang et al., 2019), photodegradation
109 (Singh et al., 2018), phytoremediation (Antoniadis et al., 2017) and microbial remediation
110 (Guan et al., 2019), have been investigated for the treatment of Ni contaminated soil and
111 water systems. In-situ stabilization methods have been widely recommended as an eco-
112 friendly and less destructive technique for the remediation of contaminated soils (Shaheen et
113 al., 2018a). Those methods involve the application of immobilizing agents to the soil matrix,
114 aiming to transform the soluble toxic element into immobile forms, making it unavailable
115 for plant uptake or translocation in the soil. Among different immobilizing agents such as
116 biosolids, lime, clays, compost, metal oxides, and animal waste (Palansooriya et al., 2020;
117 Shaheen et al., 2018a), biochar garnered high attention for the remediation of Ni
118 contaminated environments owing to its multiple environmental benefits (El-Naggar et al.,
119 2018b).

120 The utilization of biochar for the remediation of Ni contaminated soil and water has
121 been increasing over the last decade, as indicated by the steadily increasing number of
122 publications in indexed journals that deal with this hot topic (Figure 1). Biochar exhibited a
123 high immobilization efficiency for Ni in soil (Munir et al., 2020; Nawab et al., 2018;
124 Rehman et al., 2016; Shaheen et al., 2015) and aquatic systems (Zhu et al., 2019). Biochar as
125 a C-rich porous material with a high surface area, reactivity and adsorption capacity has the

126 potential to immobilize toxic elements in the soil (He et al., 2019). However, some studies
127 have reported contradictory results where biochar did not affect or decreased Ni
128 immobilization in contaminated environments (Mourgela et al., 2020; X. Yang et al., 2019).
129 Therefore, a critical review on the effectiveness of biochar for the remediation of Ni
130 contaminated soil and water is urgently needed.

131 Recently, a number of publications reviewed the potential of using biochar to
132 remediate contaminated soil and water, with most of those reviews discussing either the
133 immobilization efficiency of biochar for a group of toxic elements (Ahmad et al., 2014;
134 Bandara et al., 2020; Beesley et al., 2011; Chemerys and Baltrėnaitė, 2018; Deng et al.,
135 2020; Derakhshan Nejad et al., 2018; He et al., 2019; Rajapaksha et al., 2016; Rinklebe et al.,
136 2019) or focusing on a specific element such as arsenic (As), cadmium (Cd), copper (Cu),
137 lead (Pb), and zinc (Zn) (Li et al., 2019; Palansooriya et al., 2020; Shaaban et al., 2018;
138 Zama et al., 2018; Zhang et al., 2020). However, these reviews did not provide specific and
139 in-depth discussion for the remediation of Ni contamination in soil and water systems. The
140 sources and biogeochemical behavior of metals and their immobilization/adsorption
141 mechanisms on biochar can widely vary. Therefore, the most suitable method for biochar
142 production and modification to achieve the best performance can also greatly vary for the
143 remediation of the specific potentially toxic element, either in the soil or the water
144 environment (Shaheen et al., 2018b). Therefore, a review is needed to synthesize the
145 knowledge, draw holistic conclusions, and recommend future research directions
146 specifically for the remediation of Ni contamination. Although a large number of
147 publications (>750) have been focussed on the application of biochar (and sometimes
148 referred to as charcoal) in treating Ni-contamination (according to the Scopus database), few
149 have provided a synthesis of the current status or future perspectives in this area of research.
150 In particular, the use of pristine (unmodified) and modified (functionalized or designed)

151 biochars as immobilizing agents for Ni and the mechanisms involved have not been
152 systematically reviewed.

153 This paper synthesizes information on the different dimensions of Ni contamination,
154 the occurrence of Ni in the environment, the biogeochemistry of Ni in soil and water, the
155 potential for pristine and designer biochars to mitigate Ni contamination, and the
156 mechanisms involved in Ni remediation using biochar. We also discuss the potential risks
157 and challenges of biochar application for Ni remediation and future research perspectives.
158 This review provides state-of-the-art knowledge on Ni contamination in soil and water, and
159 the advances in biochar application as a remediation tool. We expect that this review will
160 benefit not only researchers for designing future research projects but also environmental
161 agencies and decision-makers for developing policies related to the management of Ni
162 pollution.

163

164 **2. Sources and occurrence of Ni contamination**

165 Nickel contamination occurs via disparate sources in the ecosphere, which is
166 composed of terrestrial (soil), freshwater, and marine ecosystems. Nickel is formed in the
167 soil via various lithogenic/pedogenic and anthropogenic processes; Ni contained in the soil
168 can then be transferred to ground and surface waters. The origin of Ni in a specific site plays
169 a key role in determining its biogeochemical behaviour and the proper remediation method
170 for its environmental management.

171

172 *2.1. Lithogenic/pedogenic sources of Ni contamination*

173 The type of parent material at a site affects the geochemical background of
174 potentially toxic elements in the soil. Nickel can occur naturally in the parent material; those
175 derived from pedogenic sources are affected by pedogenic soil formation processes that
176 change their concentration and distribution (Evans and Barabash, 2010). In particular,

177 weathering of soil minerals leads to chemical alteration of surfaces of primary minerals and
178 the release of more soluble forms of Ni (e.g., in association with chloride, sulphate, or
179 nitrate), which might form secondary minerals such as alumino-silicates, carbonates, oxides,
180 hydroxides, sulfates, and amorphous minerals (Massoura et al., 2006). For instance, Ni
181 contaminations in southeast Mexico and in the Mitidja plain in Algeria, were from
182 lithogenic sources such as volcanic plumes/ashes and the parent material, respectively, with
183 pedogenic processes comprising a major portion of Ni in the soil solution, containing 39-318
184 mg Ni kg⁻¹ (Hernández-Quiroz et al., 2012; Laribi et al., 2019). Nickel contamination has
185 also been reported in soils in Balkan and Serbia due to the presence of ultramafic and mafic
186 parent rocks having Ni in the range of 28-589 mg kg⁻¹ (Albanese et al., 2015; Poznanović
187 Spahić et al., 2019).

188 The spatial distribution of Ni in agricultural and grazed soils in Europe has been
189 studied (Albanese et al., 2015). Many areas in north-western Italy contained >109-114 mg
190 kg⁻¹ of Ni (Figure 2) because of the dominance of Ni-rich sedimentary rocks, alluvial
191 sediments and ophiolite complexes in that areas (Albanese et al., 2015). Sedimentary rocks
192 contain up to 90 mg kg⁻¹ of Ni (Kabata-Pendias, 2011). In general, the mineral composition
193 of parent materials has a crucial role to play in enriching Ni concentrations to > 75 mg kg⁻¹
194 in soils of many Mediterranean countries (Albanese et al., 2015). In a study on Czech
195 serpentinites, which contain 2000 to 3000 mg kg⁻¹ of Ni, Ni was highly mobile, mainly
196 released from olivine and complexes of Ni sulphide-iron oxide minerals, influenced by
197 weathering under the temperate and cold continental climates (Quantin et al., 2008).
198 Contamination of soil and water with Ni from lithogenic/pedogenic sources is usually
199 associated with parent materials that are ultramafic rocks, such as serpentinites, peridotites
200 and pyroxenites, and ophiolite outcrops (Panagopoulos et al., 2015). However, potentially
201 toxic elements in naturally contaminated soils are typically immobile and less toxic due to
202 their occurrence in the solid phase as compared to those contained in anthropogenically

203 contaminated soils (Poznanović Spahić et al., 2019). Therefore, the transfer of Ni from such
204 soils to water is limited as compared to that in anthropogenically contaminated soils.
205 Nevertheless, lithogenically/pedogenically contaminated soils still pose significant potential
206 environmental risks, in particular, under changing pH and alternating reducing-oxidizing
207 conditions, in which more labile fractions of toxic elements can be formed.

208

209 *2.2. Anthropogenic sources of Ni contamination*

210 Soil contamination of Ni from anthropogenic sources is a major threat to the
211 sustainability of our ecosystems. For instance, dust from cement and metal processing
212 industries and fly ash from fossil fuel combustion are sources of Ni at range of 91-1200 mg
213 kg⁻¹ in the soil (Panagopoulos et al., 2015; Poznanović Spahić et al., 2019). Many industrial
214 activities, such as the production of austenitic stainless steel, chemicals, and batteries, as
215 well as exhaust fumes from automobiles and refineries, are sources of Ni (Albanese et al.,
216 2015; Hernández-Quiroz et al., 2012). These industries often generate Ni-containing
217 disposals, effluents, and wastewater; those biproducts, if inappropriately discharged, could
218 pose a huge threat to soil and water contamination of Ni.

219 The Asopos river basin in Greece underwent major Ni contamination in the 1960s,
220 with Ni concentration in the contaminated sites 2.5 times higher than the baseline in the soil
221 and groundwater, mainly due to emissions from nearby activities of more than 400 industrial
222 units (Panagopoulos et al., 2015). In agricultural soils, Ni can come from fossil fuel
223 combustion, industrial discharge, mining, or smelting operations, as well as the application
224 of Ni-containing materials such as insecticides, fungicides, herbicides, and fertilizers (El-
225 Naggat et al., 2018c; Khan et al., 2017; Palansooriya et al., 2020). Therefore, soil and water
226 contamination with Ni is usually driven by anthropogenic sources with high mobility and
227 toxicity risks. Therefore, wastewater disposal was banned by law in the Asopos area

228 (Palansooriya et al., 2020; Panagopoulos et al., 2015), contaminants previously entered into
229 soil and water systems pose constant risks for the environment and human health.

230

231 *2.3. Stable isotope tracing of Ni contamination*

232 The composition of the ^{60}Ni isotope in different terrestrial samples, including
233 ultramafic soils, Fe/Mn crust, fresh water and sweater and river sediments, ranges between -
234 1.5 and 2.5‰ (Cameron and Vance, 2014; Gall et al., 2013; Ratié et al., 2015a). The source
235 of Ni in the soil can be traced using isotope analysis, since anthropogenic Ni has a higher
236 ^{60}Ni isotope composition than naturally occurring Ni (Ratié et al., 2015b). For example,
237 smelting and refining activities increased isotopic ^{60}Ni composition, which ranged between
238 0.01 and 0.20 ‰ for fly ash, and 0.11 and 0.27‰ for smelting slags, while it ranged between
239 -0.19 and 0.10 ‰ in surrounding non-ultramafic natural soils in Niquelandia, Brazil (Ratié
240 et al., 2015b). As another example, isotopic ^{60}Ni composition ranged between 0.03 and
241 0.22‰ in smelting and refining slags, while it ranged between -0.30 and 0.11 in non-
242 ultramafic soils in Barro Alto, Brazil (Ratié et al., 2015b). The isotopic ^{60}Ni composition
243 ranged between 0.56 and 1.00‰ in anthropogenic inputs (smelter slag and feeding material),
244 while it ranged between 0.22-0.49‰ in natural background (bedrock) in northeast Norway
245 (Šillerová et al., 2017). The isotopic composition of Ni can therefore be used to trace
246 anthropogenic Ni contamination in the environment.

247 Isotopic exchange kinetics for Ni also enable us to distinguish different available
248 pools of Ni via determining the rate of isotopic exchange over time (Kabata-Pendias, 2011;
249 Tongtavee et al., 2005). In this approach, the relative contribution of each Ni-bearing
250 mineral to the total Ni availability can be used to demonstrate the fractionation of available
251 Ni. Isotopically exchangeable pool of Ni is a reliable indicator of the bioavailable pool of Ni
252 in the mineral/water interface. Isotopic exchange kinetics were studied for typical Ni bearing
253 minerals such as serpentines, chlorite, smectite, goethite, and hematite (Zelano et al., 2016).

254 The rates of isotopic exchange were 100 - 1000 times higher for Ni in outer-sphere
255 complexes than that in inner-sphere complexes (Zelano et al., 2016). This phenomenon was
256 responsible for the regulation of Ni availability from Ni bearing minerals in natural samples.
257 For instance, the high abundance of the formation of outer-sphere complex sites (>80%) of
258 smectite enhanced Ni availability in the soil quickly as compared to soils rich in iron oxides;
259 whereas the formation of outer-sphere complexes was not the primary process that governs
260 Ni isotopic exchange in chlorite and deweylite. The Ni availability of pure Ni-bearing
261 minerals was successfully described via assessing the isotopic properties of ultramafic soils
262 (Echevarria, 2021).

263 Isotopically exchangeable Ni measured over time refers to the Ni retained onto soil
264 particles via sorption or surface complexation (Echevarria, 2021). The availability of Ni in
265 ultramafic soils was almost solely controlled by the abundance of Ni-bearing minerals, with
266 a limited effect by pH (Echevarria, 2021). Available Ni commonly originates from
267 secondary 2:1 clay minerals (e.g., Fe-rich smectite) and amorphous Fe oxyhydroxides
268 (Echevarria, 2021). Hence, Ni contamination is often associated with smectite-rich soils
269 formed on serpentinite, and poorly weathered Cambisols developed on peridotite under
270 temperate climates (Echevarria, 2021). The utilization of Ni isotopes for tracing the source
271 of contamination in the environment is a promising, yet challenging, approach due to the
272 scarcity of knowledge about the impact of different biogeochemical processes on the
273 isotopic fractionation of Ni (Šillerová et al., 2017).

274

275 **3. Biogeochemical behavior and environmental risks of Ni**

276 Elevated Ni concentrations over a permissible limit in soil and water pose significant
277 environmental risks, particularly if a significant portion of the element is in mobile or
278 potentially mobile fractions. The mobility and phytoavailability of Ni are dynamically
279 influenced by multiple environmental factors and processes such as pH, reducing-oxidizing

280 condition, precipitation, dissolution, complexation, ion exchange, and biological
281 transformations (Rajapaksha et al., 2018; Shaheen et al., 2018b). Geochemical fractionation
282 of Ni results in different forms of Ni in the soil, including exchangeable form and those
283 bound to carbonates, iron and manganese oxides, organic matter, and other soil fractions
284 (Tessier et al., 1979). Methods have been developed to further investigate sulfide-,
285 crystalline iron oxide-, and amorphous iron oxide-bound fractions of toxic elements (El-
286 Naggat et al., 2018c). Exchangeable and carbonate-bound fractions are considered mobile
287 fractions, non-residual fractions are considered potentially mobile when soil
288 biogeochemistry (e.g., soil pH, reduction-oxidation (redox) condition, and dissolved organic
289 carbon concentration) changes (El-Naggat et al., 2018c; Shaheen et al., 2020). The mobility
290 of toxic elements might facilitate their uptake by plants or transfer among environmental
291 compartments via soil and water routes. Soil erosion and surface runoff may lead to the
292 transfer of Ni from the soil to aquatic ecosystems and contribute to water pollution.
293 Leaching of Ni may occur, in particular, in acidic and coarse-textured soils due to the weak
294 binding between Ni and soil colloids (Palansooriya et al., 2020). Therefore, the
295 biogeochemical behavior of Ni determines their speciation, mobility and phytotoxicity in the
296 soil, bioaccumulation by plants, and transfer to the water system. Understanding the
297 biogeochemical behavior of Ni is essential to properly assess the potential environmental
298 and health risks of Ni pollution.

299

300 *3.1. Nickel in soil*

301 Nickel shows affinity with metallic Fe and S; hence, Ni-Fe and Ni-S minerals such
302 as pentlandite (Fe, Ni)₉S₈, ullmannite (NiSbS), millerite (NiS), and gersdorffite (NiAsS) are
303 formed (Albanese et al., 2015; Hooda, 2010) in the soil environment. Nickel also occurs in
304 other minerals such as kullerudite (NiSe₂), niccolite (NiAs), and ferromagnesian minerals
305 (Hooda, 2010).

306 Nickel can be mobilized during weathering of Ni-containing soil minerals via
307 different soil forming processes, and become soluble in soil solutions, allowing its
308 translocation along the soil profile (Kabata-Pendias, 2011). The mobility of Ni in soils might
309 pose a health risk as it can be moved towards the rooting zone and be taken up by plants as
310 $\text{Ni}(\text{H}_2\text{O})_6^{2+}$ (Palansooriya et al., 2020). The maximum allowable concentration of Ni in
311 agricultural soils range from 20 to 60 mg kg^{-1} , while the threshold for requiring remediation
312 ranges from 75 to 150 mg kg^{-1} (Kabata-Pendias, 2011). These values are based on a range of
313 studies and seem to be questionable due to their wide range; however, they are realistic
314 considering the variation in soil properties and Ni forms. The biogeochemical behavior and
315 forms of Ni are governed by various factors in the soil including clay type and content,
316 organic matter content and soil pH, and can be indirectly influenced by soil E_H , and the
317 content of Fe-Mn (hydr)oxides (El-Naggar et al., 2018b; Panagopoulos et al., 2015), with
318 the mobility of Ni increases under oxidizing and acidic conditions (Albanese et al., 2015; El-
319 Naggar et al., 2018c). Due to the high affinity of Ni with organic matter, the mobility of Ni
320 is dependent on soil organic matter content and composition. On the one hand, Ni binding
321 with organic ligands might diminish its mobility, as organic molecules can react with Ni to
322 create less mobile Ni forms. On the other hand, the mobility of Ni might increase with the
323 presence of fulvic and humic acids in organic matter-rich soils as those organic acids have a
324 high chelation ability (Kabata-Pendias, 2011). Nickel can co-precipitate with clay minerals
325 such as montmorillonite, which can be easily mobilized during weathering (Dähn et al.,
326 2004). Nickel can be adsorbed/complexed with soil Fe (hydro)oxides and minerals at a
327 range of 100-170 mg Ni kg^{-1} , and with soil Mn (hydro)oxides and minerals within 39-4900
328 mg Ni kg^{-1} (Kabata-Pendias, 2011). Extended X-ray absorption fine structure (EXAFS)
329 analysis on samples collected from an industrial contaminated site in southern Italy showed
330 that Ni was in a spinel-type geochemical form (trevorite; $\text{NiFe}^{3+}_2\text{O}_4$) associated with
331 magnetite and hematite (Terzano et al., 2007). The EXAFS analysis on a clayey paddy soil

332 (Ultisols) collected from Taipei City showed that Ni was incorporated into the MnO₂ layer
333 of lithiophorite in the soil (Manceau et al., 2005); this finding is in line with results from
334 Manceau et al. (2002). They demonstrated that the incorporation mechanism of Ni into the
335 MnO₂ layer might be dependent on the abundance of natural lithiophorite and the condition
336 of its formation (Manceau et al., 2005). Nickel adsorption on Fe-Mn (hydr)oxides is pH-
337 dependent, as the release of Ni into the soil solution increases with decreasing soil pH due to
338 the effect of pH on the surface charge of adsorbents in the soil (El-Naggar et al., 2018b;
339 Kabata-Pendias, 2011).

340

341 *3.2. Nickel in water*

342 Nickel is widely present in dissolved and particulate forms in natural water. The
343 dissolved forms include the hydrated divalent Ni, inorganic Ni complexes (with OH, CO₃
344 and Cl), and organic Ni complexes (i.e., Ni-humic substance inclusions), while particulate
345 forms are associated with colloids, forming larger particles (Donat et al., 1994). The
346 presence of excessive Ca and Mg can trigger the formation of weak complexes of Ni
347 (CaMgNiH₄) and the release of its bioavailable forms (NiCO₃, NiS, Ni₃S₂, NiO) that is
348 highly toxic to freshwater and marine organisms (Mandal et al., 2002). In aqueous solutions,
349 four main species of Ni, including Ni(II), Ni(OH)⁺, Ni(OH)₂ and Ni(OH)₃⁻, are formed with
350 the absence of external oxidizing agents or complete chelation for Ni (Anoop Krishnan et al.,
351 2011). The Ni(II) is the predominant form in highly acidic (pH = 0) to alkaline (pH 8.5)
352 systems (Figure 3). With increasing pH, hydroxide complexation increases and forms
353 various hydroxide species such as Ni(OH)⁺, Ni(OH)₂ and Ni(OH)₃⁻. Mainly, hydroxides of
354 nickel get phagocytised when inside the body of organisms and the Ni(II) is the actual
355 carcinogen that binds with DNA (Schaumlöffel, 2012). In aqueous solutions, Ni(II) is
356 relatively stable due to the formation of complexes with inorganic and organic ligands and
357 association with suspended soil colloids (Rinklebe and Shaheen, 2017).

358 In general, the formation of Ni-organic complexes depends mainly on the dissolved
359 organic carbon content in soil solutions or aquatic systems (El-Naggar et al., 2018c). Both
360 $\text{Ni}(\text{OH})^+$ and $\text{Ni}(\text{OH})_2$ are abundant when the pH ranges between 8.0 and 12.0, and $\text{Ni}(\text{OH})_3^-$
361 occurs mainly in highly alkaline conditions (pH = 12.0-14.0) (Anoop Krishnan et al., 2011).
362 Nickel can be rapidly sorbed on surfaces of solids when offered in the solution. For instance,
363 Ni can be adsorbed through the formation of outer-sphere complexes, in the form of
364 hydrated Ni species on the surfaces of solids. In outer-sphere complexation, the electrostatic
365 forces or H-bonding facilitates adsorption of Ni ions; therefore, they could be easily released
366 or exchanged with other ions (Rinklebe and Shaheen, 2017). On the other hand, Ni can form
367 inner-sphere complexes on the surfaces of colloids, in the form of dehydrated Ni species,
368 which are more stable (Shi et al., 2012). In water-soil systems such as wetlands, and
369 floodplains, reduction or oxidation conditions can also affect the biogeochemical behavior
370 of Ni, and its distribution among dissolved and colloidal phases (Rinklebe and Shaheen,
371 2017). Dissolved Ni concentrations were found to increase at high E_H values (oxic
372 conditions) than at low E_H values (anoxic conditions) (El-Naggar et al., 2018c). Nickel tends
373 to bound to insoluble Fe and Mn (hydr)oxides or dissolved organic matter (e.g., aromatic
374 compounds) under oxidizing conditions (El-Naggar et al., 2018c; Pyle and Couture, 2011).
375 Nickel also has an affinity to sulfates under oxic conditions, while it is commonly bound to
376 insoluble sulfides under reduced conditions; in particular, E_H -induced transformation of
377 sulfates (at high E_H values)-sulfides (at low E_H values) affected the release dynamics of Ni
378 associated with them into dissolved and colloidal phases (El-Naggar et al., 2018c).

379 However, the redox chemistry of Ni and its interactions with the solid phase and
380 colloids in aquatic systems is not sufficiently documented and requires further research to
381 understand the factors governing the mobility and redistribution of Ni among different solid-
382 water phases.

383

384 **3. Nickel remediation strategies and biochar**

385 A variety of remediation strategies has been developed to combat soil and water
386 contamination with potentially toxic elements such as Ni. Those strategies are classified into
387 physical (e.g., soil replacement, spading and washing), biological (e.g., microbial treatment
388 and phytoremediation) and chemical (electrokinetic remediation, chemical reduction,
389 chemical stabilization, and photocatalysis) technologies (Derakhshan Nejad et al., 2018; Li
390 et al., 2019; Palansooriya et al., 2020). For instance, photocatalysis is deemed a green
391 technology for the remediation of contaminated aquatic systems by converting photon
392 energy from sun light into chemical energy, and at the same time transform toxic elements
393 into nontoxic ones (Santhosh et al., 2018; Wu et al., 2020, 2018). However, the potential
394 formation of undesirable secondary products, which could be more toxic than the original
395 contaminant, via this method is a serious disadvantage (Vasilache et al., 2013). Some
396 remediation strategies aimed to permanently overcome co-existing toxic elements in the soil
397 such as soil replacement and phytoremediation. Soil replacement involves removing the
398 contaminated soil and adding a large amount of uncontaminated soil to dilute the
399 contaminant in the soil. This method is labor-demanding and has a high cost; however, it can
400 be a suitable strategy for remediating a small area of heavily contaminated soils. Utilization
401 of Ni hyperaccumulating plants such as canola (*Brassica napus* L.) for the phytoextraction
402 and removal of Ni from soil has also been reported (Adiloğlu et al., 2016; Deng et al., 2018).
403 Although phytoremediation technology can be a feasible strategy for removing Ni from
404 contaminated soils (Adiloğlu et al., 2016), it is considered an expensive and time-consuming
405 approach, and the improper management of the polluted plant can raise new environmental
406 issues (Antoniadis et al., 2017; Li et al., 2019). However, phytoremediation of Ni
407 contaminated soils is a technology that should be further explored.

408 Based on new risk-based regulatory requirements, more attention has been paid to
409 combating the potential mobility and phytoavailability of toxic elements, rather than

410 targeting the reduction of their total concentrations (Beesley et al., 2011; Zama et al., 2018).
411 Therefore, chemical stabilization technologies via the application of soil amendments to
412 immobilize toxic elements and subsequently reduce their transfer to groundwater or uptake
413 by plants have received growing interest. Remediation methods based on the in-situ
414 stabilization of contaminants are often more cost-effective, have no/minimal negative
415 impacts on soil fertility, and require simple operations (El-Naggar et al., 2020). Several
416 amendments, including clay, Fe oxides, liming materials, nanoparticles, biosolids, manure,
417 composts, coal fly ash, and biochar, have been extensively employed to immobilize toxic
418 elements in soil and water (Abbas et al., 2020; Biswas et al., 2019; Hu et al., 2015). Recent
419 studies have recommended biochar as a promising eco-friendly remediation material due to
420 its unique surface characteristics and inorganic and organic compositions (Bolan et al., 2014;
421 El-Naggar et al., 2019c, 2021; Elkhelifi et al., 2021; He et al., 2019; Man et al., 2021). In
422 particular, biochar may diminish the potential mobility and phytoavailability of Ni in the soil,
423 and play an important role in their removal from aquatic systems, as discussed in the
424 sections below.

425 Compared with the application of other restoration materials or technologies, the
426 application of biochar is superior due to its lower cost, reusability, relatively high stability
427 once reacts with the contaminant, and adaptable in the environment. In addition, biochar
428 provides various benefits such as improving soil fertility, enhancing soil water holding
429 capacity, aeration, nutrient retention and carbon sequestration, and stimulating (commonly)
430 microbial activities. Thus, biochar provides a win-win strategy for waste management and
431 climate change mitigation. Although biochar is typically more expensive than other soil
432 amendments such as compost, the lower decomposability of biochar gives it an advantage
433 over other organic amendments. For instance, once biochar is applied to farmlands, it could
434 remain in soil for decades to millennia, in contrast to compost that needs to be frequently
435 applied to maintain its effectiveness. Some argue that the pyrolysis process is costly and

436 energy-consuming, making the production of biochar a non-profitable approach in the real
437 market. This argument can be misleading as biochar production also produces various other
438 products such as bio-oil and syngas out of the same process; if the economic value of those
439 products are all realized, the cost and required energy for biochar production are diminished.
440 Therefore, biochar application for the remediation of Ni contaminated soil can be
441 economically and environmentally feasible.

442 For biochar application to remediate Ni contaminated aquatic systems, there are also
443 various approaches that could be used to augment the potentially high economic cost. For
444 example, a sequential use system which utilizes the same biochar in multiple systems can be
445 a promising approach. This approach employs the sequential application of biochar,
446 including recovering the biochar after each use, and in ideal systems, each sequence adds
447 value to the whole process. For instance, Wurzer et al. (2020) proposed the following
448 sequence for a sequential biochar use system: waste to biochar (waste management) →
449 adsorption of H₂S (biogas purification) → sulfonated catalyst (esterification) → pH
450 buffering (composting) → soil amendment (carbon sequestration). However, this being a
451 relatively new concept, the integration of the remediation of Ni contaminated aquatic
452 systems into an ideal sequential biochar use system has not been documented yet.

453

454 **4. Biochar for remediation of Ni contamination**

455 *4.1 Biochar for remediation of soil Ni contamination*

456 Numerous studies show that biochar has a high potential to immobilize Ni in the soil
457 relative to other conventional soil amendments such as limestone, organoclay, bentonite,
458 zeolite, activated-carbon, and nano-fertilizer (Shaheen et al., 2015). In Shaheen et al. (2018),
459 biochars produced from shell limestone and other substances (e.g., humus, perlite and clay)
460 were applied to a silty-acidic soil at 1% and were found to decrease water-soluble and
461 exchangeable Ni by about 59 and 34%, respectively, compared to the control treatment. In a

462 field study, hardwood biochar produced at 600 °C and applied to the soil at a range of 0.5-
463 2% resulted in up to 200% greater Ni immobilization efficiency as compared to the control,
464 three years after biochar application (Shen et al., 2016). In a pot experiment, wood biochar
465 produced at 450 °C was applied at 1 and 2% to reduce Ni bioavailability by 22 and 33%,
466 respectively, in a sandy clay loam soil with a neutral pH (Rehman et al., 2016). The
467 literature clearly demonstrated that the effectiveness of biochars for Ni remediation is
468 dependent on the feedstock type used for biochar production, while the rate of biochar
469 application had relatively small effects; however, both the feedstock type to use and the
470 application rate need to be tested for site-specific applications.

471 We extracted data from eight studies with 59 observations to evaluate the effect of
472 feedstock type, pyrolysis temperature, and biochar pH and application rate on Ni
473 immobilization efficiency (Figure 4). Biochars produced from wood and agricultural wastes
474 performed well, while manure- and sewage sludge-derived biochars had a minimal effect in
475 reducing Ni availability in the soil. Biochars produced at pyrolysis temperatures ranging
476 from 500 to 700 °C were more effective for Ni immobilization (Figure 4), consistent with
477 other studies (Shen et al., 2016; Uchimiya et al., 2012). Biochars with a high pH (9.5-10)
478 were more efficient in immobilizing Ni (Figure 4), while biochar application rate had no
479 effect on the immobilization of Ni in soil. In this case, we suggest that a low application rate
480 (<5 t ha⁻¹) would be preferable, considering the cost for biochar production, transportation,
481 and application when a high application rate is used.

482 In wetlands contaminated with Ni, the potential for biochar to immobilize Ni is
483 affected by redox dynamics. In particular, when biochar is applied to wetlands, it would
484 change soil pH due to its commonly alkaline nature, and alter soil redox potential owing to
485 its redox-active surfaces (Yuan et al., 2017). These biochar induced changes in soil pH and
486 redox potential simultaneously affect various soil properties such as dissolved
487 aliphatic/aromatic organic carbon concentrations, and the release and transformations of Fe,

488 Mn, and S/SO_4^{2-} (Rinklebe et al., 2020). The release of dissolved organic carbon and the
489 induced transformations of those elements can be accompanied by the release of associated
490 Ni from their structures and surfaces, which in turn enhances the mobility and
491 phytoavailability of Ni (El-Naggar et al., 2018c). Therefore, more research is required to
492 determine whether biochar is suitable for remediation of Ni contaminated wetlands, as
493 biochar can increase the toxicity risk of Ni under such conditions.

494 The nature of functional groups on biochar surfaces, and their potential to
495 accept/donate electrons determine biochar induced changes related to those parameters and
496 their interactions with Ni(II) in soil (El-Naggar et al., 2018c). Biochar application may also
497 affect the Ni(II) bioavailability in soil via the redistribution of Ni(II) between colloidal and
498 dissolved fractions. For example, biochars derived from shell limestone, perlite, and humus
499 decreased dissolved Ni(II) concentrations in a floodplain soil by 44%, from an average of
500 $444.5 \mu\text{g L}^{-1}$ (rang of $38.6 - 1502.9 \mu\text{g L}^{-1}$, $n=21$) in the control to average of $248.9 \mu\text{g L}^{-1}$
501 (rang of $33.5 - 683.5 \mu\text{g L}^{-1}$, $n=19$) in biochar treated soils under changing redox conditions
502 (Rinklebe et al., 2016). However, the application of rice hull biochar (pyrolyzed at 500°C)
503 increased the dissolved Ni(II) concentration by 9.5%, in particular from average of $56.3 \mu\text{g}$
504 L^{-1} (rang of $35.2 - 76.4 \mu\text{g L}^{-1}$, $n=28$) in the control to average of $61.7 \mu\text{g L}^{-1}$ (rang of $27 -$
505 $84.1 \mu\text{g L}^{-1}$, $n=32$) in biochar treated soils under dynamic redox conditions (El-Naggar et al.,
506 2018c). The variation in biochar effects on dissolved Ni(II) in those two studies was mainly
507 related to the type of biochar and soil studied. In particular, the decreased dissolved Ni in the
508 first study was associated with decreased dissolved organic carbon under an oxic condition,
509 while in the second study the biochar decreased soil pH under oxic conditions that led to the
510 acidic dissolution of Fe and Mn (hydr)oxides under aerobic-acidic conditions and the release
511 of associated Ni(II). However, there are significant knowledge gaps in the redox-mediated
512 transformation of Ni in biochar treated soils, the interactions between functional groups on
513 biochar surfaces with Ni, and the factors that control its (im)mobilization in the soil.

514 Systematic investigations are required in the future to understand the behaviour of Ni when
515 different types of biochars are applied at varying rates to different soils.

516 In summary, the potential for biochars to immobilize Ni(II) is affected by many
517 factors, including the feedstock type, pyrolysis temperature, biochar application rate, type
518 of soil, and redox conditions in the soil. The soil- and biochar property-specific nature of the
519 effect of biochar application on Ni(II) (im)mobilization needs to be further studied,
520 otherwise inappropriate biochar application may pose a critical risk of soil and water
521 contamination of Ni.

522

523 *4.2 Biochar for remediation of Ni Contamination in water*

524 Biochar has been successfully employed for the remediation of Ni contamination in
525 aquatic systems. Biochar's high porosity and surface area, and abundance of functional
526 groups play a major role in its potential to remove Ni from water, due to multiple
527 mechanisms of Ni immobilization as discussed in Section 5. However, several factors
528 influence the biochar's adsorption capacity for Ni in water. The pH of the aquatic system
529 has a major effect, and it can stimulate/inhibit the adsorption of Ni on biochar surfaces. In
530 particular, the potential for biochar to adsorb Ni increases gradually along with increasing
531 solution pH from strongly acidic to neutral (e.g., from pH 2 to 7 (Yang et al., 2019)). This is
532 attributed to pH-induced changes in biochar surface functionality. At a very low pH ($\text{pH} \leq 2$),
533 surface groups of biochar would be protonated by the solution H^+ ions, and thus there would
534 be no Ni adsorption (Bogusz et al., 2017; Yang et al., 2019). When pH increases ($\text{pH} = 2-5$),
535 deprotonation of the surface groups would occur, leading to less competition between Ni(II)
536 and H^+ ions on the binding sites of biochar surfaces; hence, Ni(II) starts to be adsorbed on
537 biochar surfaces (Higashikawa et al., 2016). At the same pH range ($\text{pH} = 2-5$), $\text{Ni}(\text{OH})^+$
538 exhibits less electrostatic repulsion with biochar surfaces, and thus, $\text{Ni}(\text{OH})^+$ would have a
539 strong electrostatic attraction on electronegative surfaces of biochars at this pH level

540 (Bogusz et al., 2017). At higher pH ($\text{pH} > 6$), the hydroxides will facilitate the precipitation
541 of Ni(II) on biochar surfaces (Shen et al., 2017). Overall, Ni can be optimally adsorbed
542 during the wastewater treatment when the pH became neutral ($\text{pH} = 7$) (Yang et al., 2019).
543 The feedstock type used for biochar production is another key factor that determines the
544 adsorption capacity of Ni in water (Figure 5). Pristine biochars produced from rice straw,
545 banana fruit waste, and orange peel have been reported to adsorb Ni(II) at concentrations of
546 54 (Deng et al., 2019), 88 (Amin et al., 2019), and 78 mg Ni g^{-1} biochar (Amin et al., 2019),
547 suggesting that those pristine biochars have a high adsorption capacity for Ni(II). Very low
548 adsorption capacities ranging from 0.22 to $1.09 \mu\text{g g}^{-1}$ were, however, reported for pristine
549 sludge and olive pomace biochars (Mourgela et al., 2020), and a water hyacinth chitosan-
550 magnetic biochar (0.48 mg g^{-1}) (Chaiyaraksa et al., 2019). The pyrolysis temperature of
551 biochar can also affect the efficiency of biochar to adsorb Ni. Biochars prepared at low
552 temperatures ($\leq 400 \text{ }^\circ\text{C}$) have low adsorption capacities, whereas those produced at high
553 temperatures ($600\text{-}800 \text{ }^\circ\text{C}$) have high capacities for removing Ni(II) from aqueous solutions.
554 For instance, biochars produced from residues of biogas production via pyrolysis at a high
555 temperature ($600 \text{ }^\circ\text{C}$) achieved higher adsorption of Ni(II) than that produced at a low
556 temperature ($400 \text{ }^\circ\text{C}$) (Bogusz et al., 2017). This is mainly attributed to higher pore volume
557 and larger specific surface area of biochar pyrolyzed at a high temperature. In general, the
558 efficiency of pristine biochars for Ni removal from aqueous solutions is highly variable as
559 they are dependent on the feedstock type and pyrolysis temperature used for their production;
560 in several cases, the adsorption capacity is low. As a result, the use of novel biochar
561 composites is becoming popular due to their high capacity for removing Ni from aqueous
562 solutions. For example, a sewage sludge biochar loaded with $\alpha\text{-Fe}_2\text{O}_3$ and $\alpha\text{-FeOOH}$
563 adsorbed $35.5 \text{ mg Ni g}^{-1}$, while unmodified sewage sludge biochar adsorbed only 20.4 mg
564 Ni g^{-1} in aqueous solutions at treatment dosage of 0.01 g biochar to 50 mL solution with 100
565 ppm initial Ni(II) concentration at neutral pH (Yang et al., 2019). A biochar produced from

566 Taihu blue algae impregnated with α -Fe₂O₃ and activated with KOH was highly efficient in
567 removing 98.8% chelated Ni at pH 6.0 (Wang et al., 2020).

568 A pine cone-alginate hybrid biochar also showed a very high Ni adsorption capacity
569 (156 mg g⁻¹) at pH 6.0 (Biswas et al., 2019). Acid and alkali modified date seed biochar also
570 adsorbed 38.7 mg Ni g⁻¹ at pH 6.0 (Mahdi et al., 2019). Similarly, a KMnO₄ and KOH
571 modified peanut shell biochar adsorbed up to 87.2 mg Ni g⁻¹ (An et al., 2019). The potential
572 for Ni removal by modified biochars was mainly governed by inner-sphere complexation of
573 Ni with oxygen-containing functional groups in biochar, and the combined effect of ion
574 exchange, electrostatic attraction, and co-precipitation. An et al. (2019) described the
575 mechanism for Ni removal as spontaneous endothermic chemisorption that was governed by
576 amine (NH₂ – Ni) and hydroxyl functional groups in biochar. The Ni removal was better
577 described by the Langmuir isotherm and pseudo-second-order kinetic models (Biswas et al.,
578 2019; Yang et al., 2019), with the Sips model (Mahdi et al., 2019) and the Freundlich
579 isotherm (Mourgela et al., 2020) also provide good fit for describing Ni removal in those
580 studies.

581 In conclusion, biochar is a promising adsorbent of Ni in contaminated aqueous
582 solutions such as industrial wastewater. Biochar surface functional groups play a major role
583 in the removal of Ni from aqueous solutions. Therefore, the application of modified biochars
584 via enriching them with functional groups such as acid/alkali groups, oxygen/amine
585 containing groups, and so on, should be a better approach than the application of pristine
586 biochar, for the remediation of Ni contaminated soil water systems.

587

588 **5. Mechanisms for the physicochemical reactions between biochar and Ni**

589 Multiple mechanisms have been suggested for the immobilization of toxic elements
590 such as Ni following biochar application; such mechanisms include ion exchange,
591 electrostatic attraction, surface complexation, (co)precipitation, physical adsorption, and

592 oxidation-reduction (Ahmad et al., 2014; He et al., 2019). We discuss below the
593 mechanisms involved in the immobilization of Ni based on the recent literature (Figure 7).

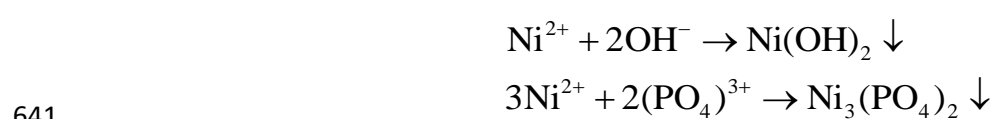
594 The adsorption of Ni(II) onto surfaces of biochars produced from sugarcane bagasse,
595 bamboo, and hickory wood chip were explained by the existence of cation- π interaction on
596 internal and external surfaces of biochars (Lyu et al., 2018). In general, ion exchange and
597 electrostatic attraction play a crucial role in the adsorption of Ni onto biochars, and could
598 lead to rapid adsorption in some cases, due to ion exchange of Ni with other cations such as
599 K^+ , Mg^{2+} , and Ca^{2+} on biochar surfaces (Yang et al., 2019).

600 Electrostatic attraction of Ni(II) by negatively charged functional groups on biochar
601 surfaces is also a potential mechanism for Ni(II) removal (Ahmad et al., 2014; El-Naggar et
602 al., 2018b), partly due to increased pH after the addition of biochar with abundant active -
603 OH functional groups on biochar surfaces (Uchimiya et al., 2010). The high
604 electronegativity of biochar depends on the variable surface negative charges, which
605 increase with pH (He et al., 2019). Batch experiments conducted using a sludge biochar
606 produced at 500 °C indicated the role of electrostatic attraction in the Ni adsorption process
607 on biochar surfaces, which gradually increased when pH increased from 2 to 7 (Yang et al.,
608 2019). The enrichment of biochar surfaces with O-containing functional groups, such as
609 carboxyl, lactonic, and hydroxyl, can decrease the surface zeta potential and the point of
610 zero charge (PZC) of biochars, hence, facilitate the Ni(II) adsorption via electrostatic
611 interaction on biochar surfaces (Lyu et al., 2018).

612 Surface functional groups, O-containing groups in particular, facilitate the binding of
613 elements and could form complexes with Ni on biochars (He et al., 2019). Biochar surfaces
614 are commonly occupied by various functional groups (eg., -COOH, -C=O, -CO- and -OH),
615 which vary with the biochar feedstock type (Figure 7). Those functional groups can be
616 altered as well based on the pyrolysis temperature used in producing the biochar (El-Naggar
617 et al., 2019b). As for biochars produced at low pyrolysis temperatures, they contain more

618 abundant functional groups on their surfaces than those prepared at high pyrolysis
619 temperatures. Complexation of Ni with O-containing functional groups on biochar surfaces
620 has been reported as a mechanism for Ni immobilization in soil (El-Naggar et al., 2018b,
621 2018c), and Ni(II) removal from contaminated aqueous solutions (Lyu et al., 2018;
622 Uchimiya et al., 2010). The addition of biochar produced from cottonseed hull at 350 °C to
623 soil significantly promoted Ni immobilization due to the predominance of O-containing
624 functional groups on biochar surfaces (Uchimiya et al., 2011). Filters made from biochars
625 reduced the Ni(II) phytotoxicity in nutrient films; filters engineered from cottonwood
626 biochar (pyrolyzed at 600 °C) scavenged the phytotoxicity of Ni(II) on tomato grown in
627 hydroponic systems, with the complexation by active functional groups (C=O and —OH in
628 particular) as a prominent mechanism (Mosa et al., 2016). Nickel(II) adsorption on surfaces
629 of wheat straw and wood pin chip biochars produced at 500-550°C were mainly attributed to
630 the coordination between Ni(II) and carboxyl and hydroxyl groups on biochar surfaces
631 (Alam et al., 2018).

632 Inorganic components in biochar may facilitate the (co)precipitation of Ni in soil or
633 water, forming insoluble precipitates such as phosphate, carbonates and (hydr)oxides. For
634 example, biochar application can induce Ni precipitation with sulfate in sediments under
635 dynamic redox conditions (El-Naggar et al., 2018c); the redox-active surfaces of biochar
636 might affect the sulphur chemistry in the soil, and consequently, Ni associated with sulfides
637 or sulfates is influenced via precipitation or release in the soil solution. Co-precipitation of
638 Ni(II) with PO_4^{3-} and OH^- , derived from biochar surfaces, was also confirmed via an
639 integrated mechanistic approach that included various chemical and spectroscopic
640 techniques and described in the following reactions.



642 Biochar application may also facilitate the precipitation of Ni with Fe, Mn, and Al, as
643 biochar application typically increases soil pH, which would decrease the dissolution of Fe,
644 Mn, and Al (hydr)oxides in acidic soils; thus it can control the mobilization or
645 immobilization of Ni associated with those minerals and oxides in soil and water systems
646 (El-Naggar et al., 2018b; Rinklebe et al., 2016).

647 Physical adsorption of Ni on internal surfaces of biochars in soil and water systems is
648 one of the mechanisms for Ni removal. Biochars can reduce the bioavailability of toxic
649 elements via sorption within their micro-pore structure (Chemerys and Baltrėnaitė, 2018).
650 Physical adsorption was a major mechanism for the high Ni adsorption capacity (up to 15.4
651 mg g⁻¹) by a corncob biochar produced at 450 °C (Hu et al., 2018). The intra-particle
652 diffusion of Ni(II) into the biochar complexed and highly variable pore system enhances the
653 potential of biochar to adsorb Ni(II) (Lyu et al., 2018). However, the pore structure and pore
654 volume affect the physical adsorption of Ni within the inner surfaces of biochar (Shaheen et
655 al., 2018b). The physical adsorption by biochar plays an important role in the remediation of
656 Ni contamination, but its contribution is less than that of chemical adsorption in remediating
657 Ni contamination (Shen et al., 2018; Yang et al., 2019). The underlying mechanisms of
658 physical adsorption of Ni in soil and water are still unclear and need to be further studied.

659 In conclusion, several mechanisms have been reported to underlie the
660 immobilization/removal of Ni in soil/aqueous solutions. Based on the literature, Ni
661 adsorption by biochar is governed by the synergistic effect of physical and chemical
662 reactions that facilitate the adsorption of Ni on biochar surfaces.

663

664 **6. Modifying biochars for immobilization of Ni in soil and water**

665 The potential for biochars to remediate Ni contamination in soil and water systems
666 depends on the chemical and physical characteristics of biochar surfaces (Shi et al., 2018),
667 which are affected by feedstock type, pyrolysis condition, and pre- and post-pyrolysis

668 modification methods used in biochar production (El-Naggar et al., 2019a). Therefore, the
669 selection of a suitable feedstock and production condition should be done before deciding on
670 a suitable modification method. Recent modification studies have attempted to increase the
671 surface area, porosity, and the abundance of active surface functional groups of biochars to
672 enhance the biochars adsorption capacity for contaminants. The efficiency for immobilizing
673 toxic elements in soil and water systems by modified biochars is greater than that of pristine
674 biochars. Here, we highlight recent advances in the field of biochar modification in order to
675 obtain biochar with superior properties and high Ni adsorption capacities (Figure 8).

676 Several physical, chemical, and biological modification methods have been reported
677 for modifying biochars for the remediation of different toxic elements. However, only a few
678 studies have attempted to modify biochars to increase their adsorption capacity for Ni. For
679 instance, biochars produced from different feedstocks (sugarcane bagasse, bamboo, and
680 hickory wood chips) and pyrolysis temperatures (300, 450, and 600 °C for a 2 h residence
681 time) were ball milled under different milling conditions (mass ratio and milling time) (Lyu
682 et al., 2018). The 12 h ball milling time and mass ratio of 1:100 biochar to ball was
683 suggested as an optimal condition to maximize the capacity of modified biochars for Ni(II)
684 adsorption (Figure 9a). The ball milling process broke down the biochar particles from
685 millimetre to submicron scale (Figure 9b-f). The ball-milled biochars exhibited higher
686 internal and external surface areas (up to a 33-fold increase), and greater acidic surface
687 functional groups (Figure 9), compared to the pristine biochars. The enhancement of these
688 acidic functional groups altered the zeta potential of the ball-milled biochar. While the zeta
689 potential for pristine biochars ranged between 24.6 and 27.9 mV, it decreased to a range
690 between -19.4 and -48.1 mV for the ball-milled biochar, with the pH ranging from 1.6 to 9.5
691 (Figure 9h). Moreover, the PZC decreased from 4 in the pristine biochar to < 0.16 in the
692 modified biochar. The ball-milled biochars had greater Ni(II) removal, faster adsorption
693 kinetics and greater capacity to adsorbed Ni(II) from aqueous solutions; the Ni(II)

694 adsorption capacity was higher than that of many commercial carbonaceous sorbents (Lyu et
695 al., 2018).

696 Sewage sludge biochars have been widely employed as adsorbents for the removal of
697 a number of toxic elements including Ni (Bogusz and Oleszczuk, 2018; Higashikawa et al.,
698 2016); however, the adsorption capacity for Ni can be enhanced when biochar is treated with
699 Fe (hydr)oxides (Yang et al., 2019). For instance, sludge biochar was produced at 500 °C
700 with a 2 h residence time, and then impregnated with $\text{FeCl}_3 \cdot 6\text{H}_2\text{O}$ and $\text{FeSO}_4 \cdot 7\text{H}_2\text{O}$
701 solutions, to be charged with Fe_2O_3 and FeOOH (Yang et al., 2019). The Fe supported
702 biochar had a surface area ($35.0 \text{ m}^2 \text{ g}^{-1}$) higher than that of pristine biochar ($24.2 \text{ m}^2 \text{ g}^{-1}$), but
703 had lower pore volume and smaller pore size, due to Fe compounds filling pores in the
704 biochar (Figure 10). The Fe-supported biochar had superior adsorption capacity for Ni (35.5
705 mg g^{-1}) compared with the pristine biochar (20.4 mg g^{-1}). The scanning electron microscopy
706 with energy dispersive x-ray (SEM-EDX) images revealed that Fe was more intensively
707 distributed on Fe-supported biochar surfaces, compared to the pristine biochar. The SEM-
708 EDX images showed that Fe and Ni were closely associated, as indicated by the locations
709 that they occupy in EDX mapping (Figure 10). This further confirms the influence of α -
710 Fe_2O_3 and α - FeOOH employed in the modification process on enhancing the biochar's
711 adsorption capacity for Ni.

712 A palm seed derived biochar-magnetic biocomposite was fabricated and tested for Ni
713 removal (Gazi et al., 2018). In order to obtain magnetic biocomposites, Fe_3O_4 was used to
714 modify biochar (Gazi et al., 2018). The biochar-magnetic biocomposite achieved removal
715 efficiency of 87% (28 mg g^{-1}) at pH 3, and up to 75% ($\sim 24 \text{ mg g}^{-1}$) in the presence of other
716 competing ions, due to its high micro-mesoporous structure. Biochar-based nanocomposites,
717 such as nanometal oxide groups, have been used to immobilize toxic elements to take
718 advantage of the benefits of both biochar and nanomaterials (El-Naggar et al., 2018b; Yang

719 et al., 2019). However, their suitability for immobilization/removal of Ni hasn't been proven
720 yet, and future studies are needed to fill this knowledge gap.

721 Surface oxidation of biochars using ammonium persulfate and hydrogen peroxide
722 has been used to increase the efficiency of biochars for Ni immobilization (El-Naggar et al.,
723 2018b). Surface oxidation of peanut hull biochar using hydrogen peroxide significantly
724 enhanced the adsorption capacity (22.8 mg g^{-1}) of Ni in contaminated water compared to
725 activated carbon (0.8 mg g^{-1}) (Xue et al., 2012). Alkali/acid treatment of biochars could also
726 increase biochars surface area and the abundance of specific functional groups. Post-
727 pyrolysis activation of wood biochar surface with sodium hydroxide, for example, increased
728 the surface area from $256 \text{ m}^2 \text{ g}^{-1}$ to $873.0 \text{ m}^2 \text{ g}^{-1}$, cation exchange capacity from 45.7 cmol
729 kg^{-1} to $124.5 \text{ cmol kg}^{-1}$, and Ni immobilization efficiency from 11 mg g^{-1} (pristine biochar)
730 to 53 mg g^{-1} (modified biochar) (Ding et al., 2016). Alkali treatment of biochar with
731 potassium hydroxide or sodium hydroxide increased the surface area and surface oxidation
732 of biochar (Rajapaksha et al., 2016). Acid activation of biochar can also increase the
733 abundance of carboxyl groups on biochar surfaces that stimulate the Ni retention in
734 immobile forms (El-Naggar et al., 2018b). Sodium sulfide as a salt of a weak acid (H_2S) and
735 a strong base (NaOH) was tried for surface modification of biochars. For example, Hu et al.
736 (2018) produced biochars at pyrolysis temperatures of 300, 450 and 600 °C using different
737 feedstocks, including crayfish shells, cotton stalks, corncob and peanut shells. They
738 modified the biochars after pyrolysis using a Na_2S solution (2 mol L^{-1}), resulting in biochars
739 with higher total pore volume that increased from 0.112 to $0.234 \text{ cm}^3 \text{ g}^{-1}$ and specific surface
740 areas increased from 11.8 to $195.6 \text{ m}^2 \text{ g}^{-1}$. Among the modified biochars, corncob biochar
741 (pyrolyzed at 450 °C) had the maximum capacity for Ni removal (15.4 mg g^{-1}) (Hu et al.,
742 2018). Enrichment of biochar surfaces with amino groups also plays an important role in
743 enhancing Ni immobilization. Corn cob biochar produced via hydrothermal carbonization
744 and modified by impregnation in a polyethylenimine solution increased the Ni adsorption

745 capacity (20 mg g^{-1}) in an aqueous solution by 43.7% as compared to the unmodified
746 biochar (Shi et al., 2018). Physical modification of biochar surfaces via steam/air activation
747 or heating was also proposed to increase the specific surface area and enhance the porous
748 structure of biochar (Rajapaksha et al., 2016), leading to increased Ni adsorption capacities
749 (El-Naggar et al., 2018b).

750 In conclusion, pristine biochars might not be efficient in the immobilization/removal
751 of Ni in highly contaminated environments. Optimization of biochar functionality and
752 characteristics via modification methods could maximize the potential of biochars for the
753 remediation of soil and water highly contaminated with Ni. Alkali/acid treatment of biochars
754 could be a promising method to increase biochar surface area and enrich surface functional
755 groups that form complexation reactions with Ni. However, some of the modification
756 methods are not eco-friendly and could even result in biochar being a source of
757 contamination, such as biochar activation using mineral acids (Lonappan et al., 2019).
758 Therefore, proper methods should be used for biochar modification. Much new research
759 needs to be done to develop effective modification methods and to investigate the long-term
760 impact of modified biochars on environmental quality and the health of organisms living in
761 the ecosystem.

762

763 **7. Conclusions and future research outlook**

764 Determining the pedogenic and anthropogenic sources of Ni and understanding
765 factors controlling their biogeochemical behaviors are of paramount importance in
766 developing a suitable tool for remediating Ni contamination. The biogeochemical behaviors
767 of Ni vary greatly with environmental conditions/characteristics, including the dynamics of
768 reduction-oxidation, biological transformation, pH, presence of multi-contaminants, the
769 chemistry of S, Fe, Mn and Al, and the content of dissolved aliphatic and aromatic carbon.
770 The biogeochemical behavior of Ni determines the speciation and the corresponding

771 mobility and toxicity of Ni in the soil, bioaccumulation in plants, and its transfer to the water
772 system. Application of biochar to Ni contaminated soil and water systems has been proven
773 to be an effective remediation tool; however, biochar effects on the mobility and
774 phytoavailability of Ni depend on the concentration and geochemistry of Ni, the
775 environment condition, and biochar characteristics. The biochar to be used for a specific site
776 for remediation of Ni contamination needs to be carefully selected, by using a suitable
777 feedstock, production condition, and pre- and post-modification treatments. Research on
778 optimization of biochar properties specifically for the immobilization of Ni in soil and water
779 is gaining increasing attention. Based on our review of the literature, the following aspects
780 need to be further studied before operational application of biochars for the remediation of
781 Ni contaminated soil and water environments and to close the knowledge gap in this area:

782

- 783 1. Environmental risk assessment must be conducted before considering large-scale
784 application of biochar to ensure that biochar application does not pose any risk to the
785 ecosystem. Different parameters, including the concentrations of potentially toxic
786 elements, polycyclic aromatic hydrocarbons, polychlorinated dibenzodioxins and
787 dibenzofurans, should be determined in the soil/water to be treated with different
788 types of pristine or modified biochars in remediation experiments.
- 789 2. Systematic investigations on the feedstock type and production condition to use for
790 the production of biochars that are effective for remediating Ni contaminated
791 environments are required. The optimization of biochar functionality via
792 modification methods would maximize the potential of biochars for the remediation
793 of soil and water contaminated with Ni. Different modification methods, however,
794 have not been systematically tested and validated for the remediation of Ni
795 contamination. Investigation on the long-term impact of modified biochars on

796 environmental quality and the health of organisms in the environment is urgently
797 needed.

798 3. Soil and water contaminated with Ni often contain other co-existing
799 organic/inorganic contaminants. Competitive adsorption among toxic elements
800 (especially among inorganic pollutants) and Ni might occur on binding sites in
801 biochars. Therefore, the sorption efficiency of modified biochars for Ni in multi-
802 contaminant environments should be tested.

803 4. The redox-mediated transformation of Ni and its interactions among the dissolved,
804 colloidal, and solid phases as affected by biochar application is still poorly
805 understood. The synergistic effects of dynamic redox conditions and biochar
806 application were found to influence the Ni forms, mobility, and phytoavailability in
807 wetlands, and floodplains, however, systematic investigations are required in the
808 future to improve our understanding of those transformation processes under
809 different soil and biochar types.

810 5. Surface oxidation of biochars via alkali/acidic activation facilitate the binding of Ni
811 on biochar. The O-containing functional groups on biochar surfaces are responsible
812 for forming specific metal-ligand complexation in soil and water systems. However,
813 the impact of this activation/modification method depends upon the feedstock type
814 and production condition of the produced biochar, and thus, studies on elucidating
815 the suitable biochar for these treatments will maximize the benefits of the biochar
816 activation on Ni retention in soil and aquatic systems.

817 6. Meta-analysis of results in the published literature on biochar application effects on
818 the remediation of Ni contamination is highly recommended and urgently needed.
819 None of the published meta-analysis studies has focused specifically on the induced
820 changes and immobilization efficiency of Ni in biochar amended soil and water
821 systems.

822 7. Finally, engineered/designer biochars have higher removal efficiencies for Ni in the
823 soil/water environment than pristine biochars. However, further research is needed to
824 validate the efficiency and superiority of engineered/designer biochars in
825 remediating Ni contamination in the soil/water environment. The strong binding of
826 Ni ions onto pristine biochar matrices reduces the desorbability of the adsorbates,
827 and hence the reusability of the spent biochar. Biochar functionalization, therefore, is
828 needed to reduce the bond energy of sorbed Ni ions on biochar, thereby increasing
829 the desorbability and recyclability of the spent biochar, particularly for the
830 remediation of Ni contaminated water, where the reuse of the spent biochar would be
831 highly desirable.

832

833 **Acknowledgements**

834 This study was supported by the National Natural Science Foundation of China
835 (42050410315, 41877085, 41877088), the Research and Development Fund of Zhejiang
836 A&F University (2018FR005, 2018FR006), the Open Research Fund Program of the State
837 Key Laboratory of Subtropical Silviculture, Zhejiang A&F University (ZY20180301,
838 ZY20180205), and the Zhejiang Postdoctoral Research Program (20120200001).

839

840 **CRedit authorship contribution statement**

841 **Ali El-Naggar**: Conceptualization, investigation, collecting review of literature, Writing -
842 original draft. **Naveed Ahmed**: Visualization, Writing - review & editing. **Ahmed Mosa**:
843 Visualization, Writing - review & editing. **Nabeel Khan Niazi**: Writing - review & editing.
844 **Balal Yousaf**: Writing - review & editing. **Anket Sharma**: Writing - review & editing.
845 **Binoy Sarkar**: Writing - review & editing. **Yanjiang Cai**: Visualization, Validation,
846 Writing - review & editing. **Scott X. Chang**: Conceptualization, Funding acquisition,
847 Supervision, Validation, Writing - review & editing.

848

849 **Declaration of Competing Interest**

850 The authors declare that they have no known competing financial interests.

851

852 **References**

- 853 Abbas, Q., Yousaf, B., Amina, Ali, M.U., Munir, M.A.M., El-Naggar, A., Rinklebe, J.,
854 Naushad, M., 2020. Transformation pathways and fate of engineered nanoparticles
855 (ENPs) in distinct interactive environmental compartments: A review. *Environ. Int.* 138,
856 105646. <https://doi.org/10.1016/j.envint.2020.105646>
- 857 Adiloğlu, S., Turgut Sağlam, M., Adiloğlu, A., Süme, A., 2016. Phytoremediation of nickel
858 (Ni) from agricultural soils using canola (*Brassica napus* L.). *Desalin. Water Treat.* 57,
859 2383–2388. <https://doi.org/10.1080/19443994.2014.994110>
- 860 Ahmad, M., Rajapaksha, A.U., Lim, J.E., Zhang, M., Bolan, N., Mohan, D., Vithanage, M.,
861 Lee, S.S., Ok, Y.S., 2014. Biochar as a sorbent for contaminant management in soil and
862 water: a review. *Chemosphere* 99, 19–33.
863 <https://doi.org/10.1016/j.chemosphere.2013.10.071>
- 864 Alam, M.S., Gorman-Lewis, D., Chen, N., Flynn, S.L., Ok, Y.S., Konhauser, K.O., Alessi,
865 D.S., 2018. Thermodynamic analysis of nickel(II) and zinc(II) adsorption to biochar.
866 *Environ. Sci. Technol.* 52, 6246–6255. <https://doi.org/10.1021/acs.est.7b06261>
- 867 Albanese, S., Sadeghi, M., Lima, A., Cicchella, D., Dinelli, E., Valera, P., Falconi, M.,
868 Demetriades, A., De Vivo, B., Etc., 2015. GEMAS: Cobalt, Cr, Cu and Ni distribution
869 in agricultural and grazing land soil of Europe. *J. Geochem. Explor* 154, 81–93.
870 <https://doi.org/10.1016/j.gexplo.2015.01.004>
- 871 Amin, M.T., Alazba, A.A., Shafiq, M., 2019. Comparative sorption of nickel from an
872 aqueous solution using biochar derived from banana and orange peel using a batch
873 system: Kinetic and isotherm models. *Arab. J. Sci. Eng.* 44, 10105–10116.

874 <https://doi.org/10.1007/s13369-019-03907-6>

875 An, Q., Jiang, Y.Q., Nan, H.Y., Yu, Y., Jiang, J.N., 2019. Unraveling sorption of nickel
876 from aqueous solution by KMnO₄ and KOH-modified peanut shell biochar: Implicit
877 mechanism. *Chemosphere* 214, 846–854.
878 <https://doi.org/10.1016/j.chemosphere.2018.10.007>

879 Anoop Krishnan, K., Sreejalekshmi, K.G., Baiju, R.S., 2011. Nickel(II) adsorption onto
880 biomass based activated carbon obtained from sugarcane bagasse pith. *Bioresour.*
881 *Technol.* 102, 10239–10247. <https://doi.org/10.1016/j.biortech.2011.08.069>

882 Antoniadis, V., Levizou, E., Shaheen, S.M., Ok, Y.S., Sebastian, A., Baum, C., Prasad,
883 M.N.V., Wenzel, W.W., Rinklebe, J., 2017. Trace elements in the soil-plant interface:
884 Phytoavailability, translocation, and phytoremediation—A review. *Earth-Science Rev.*
885 171, 621–645. <https://doi.org/10.1016/J.EARSCIREV.2017.06.005>

886 Babaahmadifooladi, M., Jacxsens, L., De Meulenaer, B., Du Laing, G., 2020. Nickel in
887 foods sampled on the Belgian market: identification of potential contamination sources.
888 *Food Addit. Contam. - Part A Chem. Anal. Control. Expo. Risk Assess.* 37, 607–621.
889 <https://doi.org/10.1080/19440049.2020.1714751>

890 Bandara, T., Franks, A., Xu, J., Bolan, N., Wang, H., Tang, C., 2020. Chemical and
891 biological immobilization mechanisms of potentially toxic elements in biochar-
892 amended soils. *Crit. Rev. Environ. Sci. Technol.* 50, 903–978.
893 <https://doi.org/10.1080/10643389.2019.1642832>

894 Beesley, L., Moreno-Jiménez, E., Gomez-Eyles, J.L., Harris, E., Robinson, B., Sizmur, T.,
895 2011. A review of biochars' potential role in the remediation, revegetation and
896 restoration of contaminated soils. *Environ. Pollut.* 159, 3269–3282.
897 <https://doi.org/10.1016/j.envpol.2011.07.023>

898 Biswas, S., Meikap, B.C., Sen, T.K., 2019. Adsorptive removal of aqueous phase copper
899 (Cu²⁺) and nickel (Ni²⁺) metal ions by synthesized biochar–biopolymeric hybrid

900 adsorbents and process optimization by response surface methodology (RSM). *Water.*
901 *Air. Soil Pollut.* 230, 1–23. <https://doi.org/10.1007/s11270-019-4258-y>

902 Bogusz, A., Nowak, K., Stefaniuk, M., Dobrowolski, R., Oleszczuk, P., 2017. Synthesis of
903 biochar from residues after biogas production with respect to cadmium and nickel
904 removal from wastewater. *J. Environ. Manage.* 201, 268–276.
905 <https://doi.org/10.1016/j.jenvman.2017.06.019>

906 Bogusz, A., Oleszczuk, P., 2018. Sequential extraction of nickel and zinc in sewage sludge-
907 or biochar/sewage sludge-amended soil. *Sci. Total Environ.* 636, 927–935.
908 <https://doi.org/10.1016/j.scitotenv.2018.04.072>

909 Bolan, N., Kunhikrishnan, A., Thangarajan, R., Kumpiene, J., Park, J., Makino, T., Kirkham,
910 M.B., Scheckel, K., 2014. Remediation of heavy metal(loid)s contaminated soils - To
911 mobilize or to immobilize? *J. Hazard. Mater.* 266, 141–166.
912 <https://doi.org/10.1016/j.jhazmat.2013.12.018>

913 Cameron, V., Vance, D., 2014. Heavy nickel isotope compositions in rivers and the oceans.
914 *Geochim. Cosmochim. Acta* 128, 195–211. <https://doi.org/10.1016/j.gca.2013.12.007>

915 Chaiyaraksa, C., Boonyakiat, W., Bukkontod, W., Ngakom, W., 2019. Adsorption of copper
916 (II) and nickel (II) by chemical modified magnetic biochar derived from eichhornia
917 crassipes. *Environment Asia* 12, 14–23. <https://doi.org/10.14456/ea.2019.23>

918 Chemerys, V., Baltrėnaitė, E., 2018. A review of lignocellulosic biochar modification
919 towards enhanced biochar selectivity and adsorption capacity of potentially toxic
920 elements. *Ukr. J. Ecol.* 8, 21–32. https://doi.org/10.15421/2018_183

921 Cheng, S.Y., Show, P.L., Lau, B.F., Chang, J.S., Ling, T.C., 2019. New prospects for
922 modified algae in heavy metal adsorption. *Trends Biotechnol.* 37, 1255–1268.
923 <https://doi.org/10.1016/j.tibtech.2019.04.007>

924 Dähn, R., Schneidegger, A.M., Manceau, A., 2004. Uptake mechanisms of Ni(II) on
925 montmorillonite as determined by X-ray absorption spectroscopy (abstr.). *Goldschmidt.*

926 Deng, R., Huang, D., Wan, J., Xue, W., Wen, X., Liu, X., Chen, S., Lei, L., Zhang, Q., 2020.
927 Recent advances of biochar materials for typical potentially toxic elements
928 management in aquatic environments: A review. *J. Clean. Prod.* 255, 119523.
929 <https://doi.org/10.1016/j.jclepro.2019.119523>

930 Deng, T.H.B., van der Ent, A., Tang, Y.T., Sterckeman, T., Echevarria, G., Morel, J.L., Qiu,
931 R.L., 2018. Nickel hyperaccumulation mechanisms: a review on the current state of
932 knowledge. *Plant Soil.* 423, 1–11. <https://doi.org/10.1007/s11104-017-3539-8>

933 Deng, Y., Huang, S., Laird, D.A., Wang, X., Meng, Z., 2019. Adsorption behaviour and
934 mechanisms of cadmium and nickel on rice straw biochars in single- and binary-metal
935 systems. *Chemosphere* 218, 308–318.
936 <https://doi.org/10.1016/j.chemosphere.2018.11.081>

937 Derakhshan Nejad, Z., Jung, M.C., Kim, K.H., 2018. Remediation of soils contaminated
938 with heavy metals with an emphasis on immobilization technology. *Environ. Geochem.*
939 *Health.* 40, 927–953. <https://doi.org/10.1007/s10653-017-9964-z>

940 Di Palma, L., Gueye, M.T., Petrucci, E., 2015. Hexavalent chromium reduction in
941 contaminated soil: A comparison between ferrous sulphate and nanoscale zero-valent
942 iron. *J. Hazard. Mater.* 281, 70–76. <https://doi.org/10.1016/j.jhazmat.2014.07.058>

943 Ding, Z., Hu, X., Wan, Y., Wang, S., Gao, B., 2016. Removal of lead, copper, cadmium,
944 zinc, and nickel from aqueous solutions by alkali-modified biochar: Batch and column
945 tests. *J. Ind. Eng. Chem.* 33, 239–245. <https://doi.org/10.1016/j.jiec.2015.10.007>

946 Donat, J.R., Lao, K.A., Bruland, K.W., 1994. Speciation of dissolved copper and nickel in
947 South San Francisco Bay: a multi-method approach. *Anal. Chim. Acta* 284, 547–571.
948 [https://doi.org/10.1016/0003-2670\(94\)85061-5](https://doi.org/10.1016/0003-2670(94)85061-5)

949 Echevarria, Guillaume, 2021. Genesis and behaviour of ultramafic soils and consequences
950 for nickel biogeochemistry, in: van der Ent, A., Baker, A.J., Echevarria, G., Simonnot,
951 M., Morel, J.L. (Eds.), *Agromining: Farming for Metals. Mineral Resource Reviews.*

952 Springer, Cham, pp. 215–238. https://doi.org/10.1007/978-3-030-58904-2_11

953 Eissa, M.A., 2019. Effect of cow manure biochar on heavy metals uptake and translocation
954 by zucchini (*Cucurbita pepo* L). *Arab. J. Geosci.* 12, 48.
955 <https://doi.org/10.1007/s12517-018-4191-1>

956 El-Naggar, A., El-Naggar, A.H., Shaheen, S.M., Sarkar, B., Chang, S.X., Tsang, D.C.W.,
957 Rinklebe, J., Ok, Y.S., 2019a. Biochar composition-dependent impacts on soil nutrient
958 release, carbon mineralization, and potential environmental risk: A review. *J. Environ.*
959 *Manage.* 241, 1–10. <https://doi.org/10.1016/j.jenvman.2019.02.044>

960 El-Naggar, A., Lee, M.H., Hur, J., Lee, Y.H., Igalavithana, A.D., Shaheen, S.M., Ryu, C.,
961 Rinklebe, J., Tsang, D.C.W., Ok, Y.S., 2020. Biochar-induced metal immobilization
962 and soil biogeochemical process: An integrated mechanistic approach. *Sci. Total*
963 *Environ.* 698, 134112. <https://doi.org/10.1016/j.scitotenv.2019.134112>

964 El-Naggar, A., Lee, S.S., Awad, Y.M., Yang, X., Ryu, C., Rizwan, M., Rinklebe, J., Tsang,
965 D.C.W., Ok, Y.S., 2018a. Influence of soil properties and feedstocks on biochar
966 potential for carbon mineralization and improvement of infertile soils. *Geoderma* 332,
967 100–108. <https://doi.org/10.1016/j.geoderma.2018.06.017>

968 El-Naggar, A., Lee, S.S., Rinklebe, J., Farooq, M., Song, H., Sarmah, A.K., Zimmerman,
969 A.R., Ahmad, M., Shaheen, S.M., Ok, Y.S., 2019b. Biochar application to low fertility
970 soils: A review of current status, and future prospects. *Geoderma* 337, 536–554.
971 <https://doi.org/10.1016/j.geoderma.2018.09.034>

972 El-Naggar, A., Rajapaksha, A.U., Shaheen, S.M., Rinklebe, J., Ok, Y.S., 2018b. Potential of
973 biochar to immobilize nickel in contaminated soils, in: *Nickel in Soils and Plants*. CRC
974 Press, pp. 293–318. <https://doi.org/10.1201/9781315154664-13>

975 El-Naggar, A., Shaheen, S.M., Chang, S.X., Hou, D., Ok, Y.S., Rinklebe, J., 2021. Biochar
976 surface functionality plays a vital role in (im)mobilization and phytoavailability of soil
977 vanadium. *ACS Sustain. Chem. Eng.* 9, 6864–6874.

978 <https://doi.org/10.1021/acssuschemeng.1c01656>

979 El-Naggar, A., Shaheen, S.M., Ok, Y.S., Rinklebe, J., 2018c. Biochar affects the dissolved
980 and colloidal concentrations of Cd, Cu, Ni, and Zn and their phytoavailability and
981 potential mobility in a mining soil under dynamic redox-conditions. *Sci. Total Environ.*
982 624, 1059–1071. <https://doi.org/10.1016/j.scitotenv.2017.12.190>

983 El-Naggar, A., Shaheen, S.M.S.M., Hseu, Z.-Y.Z.-Y., Wang, S.-L.S.-L., Ok, Y.S.Y.S.,
984 Rinklebe, J., 2019c. Release dynamics of As, Co, and Mo in a biochar treated soil
985 under pre-definite redox conditions. *Sci. Total Environ.* 657, 686–695.
986 <https://doi.org/10.1016/J.SCITOTENV.2018.12.026>

987 Elkhilifi, Z., Kamran, M., Maqbool, A., El-Naggar, A., Ifthikar, J., Parveen, A., Bashir, S.,
988 Rizwan, M., Mustafa, A., Irshad, S., Ali, S., Chen, Z., 2021. Phosphate-lanthanum
989 coated sewage sludge biochar improved the soil properties and growth of ryegrass in an
990 alkaline soil. *Ecotoxicol. Environ. Saf.* 216, 112173.
991 <https://doi.org/10.1016/j.ecoenv.2021.112173>

992 Evans, L.J., Barabash, S.J., 2010. Molybdenum, silver, thallium and vanadium, in: *Trace*
993 *Elements in Soils*. pp. 515–549. <https://doi.org/10.1002/9781444319477.ch22>

994 Fiyadh, S.S., AlSaadi, M.A., Jaafar, W.Z., AlOmar, M.K., Fayaed, S.S., Mohd, N.S., Hin,
995 L.S., El-Shafie, A., 2019. Review on heavy metal adsorption processes by carbon
996 nanotubes. *J. Clean. Prod.* 230, 783–793. <https://doi.org/10.1016/j.jclepro.2019.05.154>

997 Gall, L., Williams, H.M., Siebert, C., Halliday, A.N., Herrington, R.J., Hein, J.R., 2013.
998 Nickel isotopic compositions of ferromanganese crusts and the constancy of deep ocean
999 inputs and continental weathering effects over the Cenozoic. *Earth Planet. Sci. Lett.*
1000 375, 148–155. <https://doi.org/10.1016/j.epsl.2013.05.019>

1001 Gazi, M., Oladipo, A.A., Azalok, K.A., 2018. Highly efficient and magnetically separable
1002 palm seed-based biochar for the removal of nickel. *Sep. Sci. Technol.* 53, 1124–1131.
1003 <https://doi.org/10.1080/01496395.2017.1340955>

1004 Gonnelli, C., Renella, G., 2013. Chromium and nickel, in: Alloway B. (Ed.), Heavy Metals
1005 in Soils: Trace Metals and Metalloids in Soils and Their Bioavailability. Springer,
1006 Dordrecht. https://doi.org/10.1007/978-94-007-4470-7_11

1007 Guan, C.Y., Tseng, Y.H., Tsang, D.C.W., Hu, A., Yu, C.P., 2019. Wetland plant microbial
1008 fuel cells for remediation of hexavalent chromium contaminated soils and electricity
1009 production. *J. Hazard. Mater.* 365, 137–145.
1010 <https://doi.org/10.1016/j.jhazmat.2018.10.086>

1011 He, L., Zhong, H., Liu, G., Dai, Z., Brookes, P.C., Xu, J., 2019. Remediation of heavy metal
1012 contaminated soils by biochar: Mechanisms, potential risks and applications in China.
1013 *Environ. Pollut.* 252, 846–855. <https://doi.org/10.1016/j.envpol.2019.05.151>

1014 Hernández-Quiroz, M., Herre, A., Cram, S., de León, C.P., Siebe, C., 2012. Pedogenic,
1015 lithogenic - or anthropogenic origin of Cr, Ni and V in soils near a petrochemical
1016 facility in Southeast Mexico. *Catena* 93, 49–57.
1017 <https://doi.org/10.1016/j.catena.2012.01.005>

1018 Higashikawa, F.S., Conz, R.F., Colzato, M., Cerri, C.E.P., Alleoni, L.R.F., 2016. Effects of
1019 feedstock type and slow pyrolysis temperature in the production of biochars on the
1020 removal of cadmium and nickel from water. *J. Clean. Prod.* 137, 965–972.
1021 <https://doi.org/10.1016/j.jclepro.2016.07.205>

1022 Hooda, P.S., 2010. Trace Elements in Soils, Trace Elements in Soils. Wiley.
1023 <https://doi.org/10.1002/9781444319477>

1024 Hu, X., He, M., Kong, L., 2015. Photopromoted oxidative dissolution of stibnite. *Appl.*
1025 *Geochemistry* 61, 53–61. <https://doi.org/10.1016/j.apgeochem.2015.05.014>

1026 Hu, X., Xue, Y., Liu, L., Zeng, Y., Long, L., 2018. Preparation and characterization of
1027 Na₂S-modified biochar for nickel removal. *Environ. Sci. Pollut. Res.* 25, 9887–9895.
1028 <https://doi.org/10.1007/s11356-018-1298-6>

1029 Hussain, J., Husain, I., Arif, M., Gupta, N., 2017. Studies on heavy metal contamination in

1030 Godavari river basin. *Appl. Water Sci.* 7, 4539–4548.

1031 Ibrahim, M., Li, G., Chan, F.K.S., Kay, P., Liu, X.-X., Firbank, L., Xu, Y.-Y., 2019.

1032 Biochars effects potentially toxic elements and antioxidant enzymes in *Lactuca sativa*

1033 L. grown in multi-metals contaminated soil. *Environ. Technol. Innov.* 15, 100427.

1034 <https://doi.org/10.1016/j.eti.2019.100427>

1035 Kabata-Pendias, A., 2011. *Trace Elements in Soils and Plants*. CRC Press. ISBN

1036 9781420093681

1037 Khan, M.N., Mobin, M., Abbas, Z.K., Alamri, S.A., 2017. Fertilizers and their contaminants

1038 in soils, surface and groundwater, in: *Encyclopedia of the Anthropocene*. Elsevier, pp.

1039 225–240. <https://doi.org/10.1016/B978-0-12-809665-9.09888-8>

1040 Laribi, A., Shand, C., Wendler, R., Mouhouche, B., Colinet, G., 2019. Concentrations and

1041 sources of Cd, Cr, Cu, Fe, Ni, Pb and Zn in soil of the Mitidja plain, Algeria. *Toxicol.*

1042 *Environ. Chem.* 101, 59–74. <https://doi.org/10.1080/02772248.2019.1619744>

1043 Li, C., Zhou, K., Qin, W., Tian, C., Qi, M., Yan, X., Han, W., 2019. A Review on heavy

1044 metals contamination in soil: Effects, sources, and remediation techniques. *Soil*

1045 *Sediment Contam.* 28, 380–394. <https://doi.org/10.1080/15320383.2019.1592108>

1046 Lonappan, L., Liu, Y., Rouissi, T., Brar, S.K., Surampalli, R.Y., 2019. Development of

1047 biochar-based green functional materials using organic acids for environmental

1048 applications. *J. Clean. Prod.* 244, 118841. <https://doi.org/10.1016/j.jclepro.2019.118841>

1049 Lyu, H., Gao, B., He, F., Zimmerman, A.R., Ding, C., Huang, H., Tang, J., 2018. Effects of

1050 ball milling on the physicochemical and sorptive properties of biochar: Experimental

1051 observations and governing mechanisms. *Environ. Pollut.* 233, 54–63.

1052 <https://doi.org/10.1016/j.envpol.2017.10.037>

1053 Mahdi, Z., El Hanandeh, A., Yu, Q.J., 2019. Preparation, characterization and application of

1054 surface modified biochar from date seed for improved lead, copper, and nickel removal

1055 from aqueous solutions. *J. Environ. Chem. Eng.* 7, 103379.

1056 <https://doi.org/10.1016/j.jece.2019.103379>

1057 Man, Y., Wang, B., Wang, J., Slaný, M., Yan, H., Li, P., El-Naggar, A., Shaheen, S.M.,
1058 Rinklebe, J., Feng, X., 2021. Use of biochar to reduce mercury accumulation in *Oryza*
1059 *sativa* L: A trial for sustainable management of historically polluted farmlands. Environ.
1060 Int. 153, 106527. <https://doi.org/10.1016/j.envint.2021.106527>

1061 Manceau, A., Tamura, N., Marcus, M.A., MacDowell, A.A., Celestre, R.S., Sublett, R.E.,
1062 Sposito, G., Padmore, H.A., 2002. Deciphering Ni sequestration in soil ferromanganese
1063 nodules by combining X-ray fluorescence, absorption, and diffraction at micrometer
1064 scales of resolution. Am. Mineral. 87, 1494–1499. [https://doi.org/10.2138/am-2002-](https://doi.org/10.2138/am-2002-1028)
1065 1028

1066 Manceau, A., Tommaseo, C., Rihs, S., Geoffroy, N., Chateigner, D., Schlegel, M., Tisserand,
1067 D., Marcus, M.A., Tamura, N., Chen, Z.S., 2005. Natural speciation of Mn, Ni, and Zn
1068 at the micrometer scale in a clayey paddy soil using X-ray fluorescence, absorption,
1069 and diffraction. Geochim. Cosmochim. Acta 69, 4007–4034.
1070 <https://doi.org/10.1016/j.gca.2005.03.018>

1071 Mandal, R., Hassan, N.M., Murimboh, J., Chakrabarti, C.L., Back, M.H., Rahayu, U., Lean,
1072 D.R.S., 2002. Chemical speciation and toxicity of nickel species in natural waters from
1073 the sudbury area (Canada). Environ. Sci. Technol. 36, 1477–1484.
1074 <https://doi.org/10.1021/es015622e>

1075 Massoura, S.T., Echevarria, G., Becquer, T., Ghanbaja, J., Leclerc-Cessac, E., Morel, J.-L.,
1076 2006. Control of nickel availability by nickel bearing minerals in natural and
1077 anthropogenic soils. Geoderma 136, 28–37.
1078 <https://doi.org/10.1016/j.geoderma.2006.01.008>

1079 Mosa, A., El-Banna, M.F., Gao, B., 2016. Biochar filters reduced the toxic effects of nickel
1080 on tomato (*Lycopersicon esculentum* L.) grown in nutrient film technique hydroponic
1081 system. Chemosphere. 149, 254–62. <https://doi.org/10.1016/j.chemosphere.2016.01.104>

1082 Mourgela, R.N., Regkouzas, P., Pelleri, F.M., Diamadopoulos, E., 2020. Ni(II) adsorption
1083 on biochars produced from different types of biomass. *Water. Air. Soil Pollut.* 231, 1–
1084 16. <https://doi.org/10.1007/s11270-020-04591-1>

1085 Munir, M.A.M., Liu, G., Yousaf, B., Mian, M.M., Ali, M.U., Ahmed, R., Cheema, A.I.,
1086 Naushad, M., 2020. Contrasting effects of biochar and hydrothermally treated coal
1087 gangue on leachability, bioavailability, speciation and accumulation of heavy metals by
1088 rapeseed in copper mine tailings. *Ecotoxicol. Environ. Saf.* 191, 110244.
1089 <https://doi.org/10.1016/j.ecoenv.2020.110244>

1090 Nawab, J., Ghani, J., Khan, S., Xiaoping, W., 2018. Minimizing the risk to human health
1091 due to the ingestion of arsenic and toxic metals in vegetables by the application of
1092 biochar, farmyard manure and peat moss. *J. Environ. Manage.* 214, 172–183.
1093 <https://doi.org/10.1016/j.jenvman.2018.02.093>

1094 Palansooriya, K.N., Shaheen, S.M., Chen, S.S., Tsang, D.C.W., Hashimoto, Y., Hou, D.,
1095 Bolan, N.S., Rinklebe, J., Ok, Y.S., 2020. Soil amendments for immobilization of
1096 potentially toxic elements in contaminated soils: A critical review. *Environ. Int.* 134,
1097 105046. <https://doi.org/10.1016/j.envint.2019.105046>

1098 Panagopoulos, I., Karayannis, A., Kollias, K., Xenidis, A., Papassiopi, N., 2015.
1099 Investigation of potential soil contamination with Cr and Ni in four metal finishing
1100 facilities at Asopos industrial area. *J. Hazard. Mater.* 281, 20–26.
1101 <https://doi.org/10.1016/j.jhazmat.2014.07.040>

1102 Parades-Aguilar, J., Reyes-Martínez, V., Bustamante, G., Almendáriz-Tapia, F.J., Martínez-
1103 Meza, G., Vílchez-Vargas, R., Link, A., Certucha-Barragán, M.T., Calderón, K., 2021.
1104 Removal of nickel(II) from wastewater using a zeolite-packed anaerobic bioreactor:
1105 Bacterial diversity and community structure shifts. *J. Environ. Manage.* 279, 111558.
1106 <https://doi.org/10.1016/j.jenvman.2020.111558>

1107 Poznanović Spahić, M.M., Sakan, S.M., Glavaš-Trbić, B.M., Tančić, P.I., Škrivanj, S.B.,

1108 Kovačević, J.R., Manojlović, D.D., 2019. Natural and anthropogenic sources of
1109 chromium, nickel and cobalt in soils impacted by agricultural and industrial activity
1110 (Vojvodina, Serbia). *J. Environ. Sci. Heal. - Part A Toxic/Hazardous Subst. Environ.*
1111 *Eng.* 54, 219–230. <https://doi.org/10.1080/10934529.2018.1544802>

1112 Pyle, G., Couture, P., 2011. Nickel, in: Wood, C.M., Farrell A.P., Brauner, C.J. (Eds.),
1113 Homeostasis and Toxicology of Essential Metals. *Fish Physiology*. Academic Press. 31,
1114 253–289. [https://doi.org/10.1016/S1546-5098\(11\)31005-9](https://doi.org/10.1016/S1546-5098(11)31005-9)

1115 Quantin, C., Ettler, V., Garnier, J., Šebek, O., 2008. Sources and extractibility of chromium
1116 and nickel in soil profiles developed on Czech serpentinites. *Comptes Rendus - Geosci.*
1117 340, 872–882. <https://doi.org/10.1016/j.crte.2008.07.013>

1118 Rajapaksha, A.U., Alam, M.S., Chen, N., Alessi, D.S., Igalavithana, A.D., Tsang, D.C.W.,
1119 Ok, Y.S., 2018. Removal of hexavalent chromium in aqueous solutions using biochar:
1120 Chemical and spectroscopic investigations. *Sci. Total Environ.* 625, 1567–1573.
1121 <https://doi.org/10.1016/j.scitotenv.2017.12.195>

1122 Rajapaksha, A.U., Chen, S.S., Tsang, D.C.W., Zhang, M., Vithanage, M., Mandal, S., Bolan,
1123 N.S., Sik Ok, Y., 2016. Engineered/designer biochar for contaminant
1124 removal/immobilization from soil and water: Potential and implication of biochar
1125 modification. *Chemosphere* 148, 276–291.
1126 <https://doi.org/10.1016/j.chemosphere.2016.01.043>

1127 Ratić, G., Jouvin, D., Garnier, J., Rouxel, O., Miska, S., Guimarães, E., Cruz Vieira, L.,
1128 Sivry, Y., Zelano, I., Montarges-Pelletier, E., Thil, F., Quantin, C., 2015a. Nickel
1129 isotope fractionation during tropical weathering of ultramafic rocks. *Chem. Geol.* 402,
1130 68–76. <https://doi.org/10.1016/j.chemgeo.2015.02.039>

1131 Ratić, G., Quantin, C., Jouvin, D., Calmels, D., Ettler, V., Sivry, Y., Vieira, L.C., Ponzevera,
1132 E., Garnier, J., 2015b. Nickel isotope fractionation during laterite Ni ore smelting and
1133 refining: Implications for tracing the sources of Ni in smelter-affected soils. *Appl.*

1134 Geochemistry 64, 136–145. <https://doi.org/10.1016/j.apgeochem.2015.09.005>

1135 Rehman, M.Z.U., Rizwan, M., Ali, S., Fatima, N., Yousaf, B., Naeem, A., Sabir, M., Ahmad,
1136 H.R., Ok, Y.S., 2016. Contrasting effects of biochar, compost and farm manure on
1137 alleviation of nickel toxicity in maize (*Zea mays* L.) in relation to plant growth,
1138 photosynthesis and metal uptake. *Ecotoxicol. Environ. Saf.* 133, 218–225.
1139 <https://doi.org/10.1016/j.ecoenv.2016.07.023>

1140 Rinklebe, J., Antoniadis, V., Shaheen, S.M., Rosche, O., Altermann, M., 2019. Health risk
1141 assessment of potentially toxic elements in soils along the Central Elbe River, Germany.
1142 *Environ. Int.* 126, 76–88. <https://doi.org/10.1016/J.ENVINT.2019.02.011>

1143 Rinklebe, J., Shaheen, S.M., 2017. Redox chemistry of nickel in soils and sediments: A
1144 review. *Chemosphere* 179, 265–278.
1145 <https://doi.org/10.1016/j.chemosphere.2017.02.153>

1146 Rinklebe, J., Shaheen, S.M., El-Naggar, A., Wang, H., Du Laing, G., Alessi, D.S., Sik Ok,
1147 Y., 2020. Redox-induced mobilization of Ag, Sb, Sn, and Tl in the dissolved, colloidal
1148 and solid phase of a biochar-treated and un-treated mining soil. *Environ. Int.* 140,
1149 105754. <https://doi.org/10.1016/j.envint.2020.105754>

1150 Rinklebe, J., Shaheen, S.M., Frohne, T., 2016. Amendment of biochar reduces the release of
1151 toxic elements under dynamic redox conditions in a contaminated floodplain soil.
1152 *Chemosphere* 142, 41–47. <https://doi.org/10.1016/j.chemosphere.2015.03.067>

1153 Rodríguez-Vila, A., Covelo, E.F., Forján, R., Asensio, V., 2015. Recovering a copper mine
1154 soil using organic amendments and phytomanagement with *Brassica juncea* L. J.
1155 *Environ. Manage.* 147, 73–80. <https://doi.org/10.1016/j.jenvman.2014.09.011>

1156 Russell, R.M., Beard, J.L., Cousins, R.J., Dunn, J.T., Ferland, G., Hambidge, K.M., Lynch,
1157 S., Penland, J.G., Ross, A.C., Stoecker, B.J., 2001. Dietary reference intakes for
1158 vitamin A, vitamin K, arsenic, boron, chromium, copper, iodine, iron, manganese,
1159 molybdenum, nickel, silicon, vanadium, and zinc. A Rep. Panel Micronutr. Subcomm.

1160 Up. Ref. Levels Nutr. Interpret. Uses Diet. Ref. Intakes, Standing Comm. Sci. Eval.
1161 Diet. Ref. Intakes Food Nutr.

1162 Samantaray, P.K., Madras, G., Bose, S., 2019. Microbial biofilm membranes for water
1163 remediation and photobiocatalysis. ACS Symp. Ser. 1329, 321–351.
1164 <https://doi.org/10.1021/bk-2019-1329.ch014>

1165 Santhosh, C., Malathi, A., Daneshvar, E., Kollu, P., Bhatnagar, A., 2018. Photocatalytic
1166 degradation of toxic aquatic pollutants by novel magnetic 3D-TiO₂@HPGA
1167 nanocomposite. Sci. Rep. 8, 1–15. <https://doi.org/10.1038/s41598-018-33818-9>

1168 Schaumlöffel, D., 2012. Nickel species: Analysis and toxic effects. J. Trace Elem. Med. Biol.
1169 26, 1–6. <https://doi.org/https://doi.org/10.1016/j.jtemb.2012.01.002>

1170 Shaaban, M., Van Zwieten, L., Bashir, S., Younas, A., Núñez-Delgado, A., Chhajro, M.A.,
1171 Kubar, K.A., Ali, U., Rana, M.S., Mehmood, M.A., Hu, R., 2018. A concise review of
1172 biochar application to agricultural soils to improve soil conditions and fight pollution. J.
1173 Environ. Manage. 228, 429–440. <https://doi.org/10.1016/j.jenvman.2018.09.006>

1174 Shaheen, S.M., Antić-Mladenović, S., Wang, S.-L., Niazi, N.K., Tsadilas, C.D., Ok, Y.S.,
1175 Rinklebe, J., 2018a. Nickel mobilization/immobilization and phytoavailability in soils
1176 as affected by organic and inorganic amendments, in: Tsadilas, C., Rinklebe, J. (Eds.),
1177 Nickel in Soils and Plants. CRC Press, Taylor & Francis Group, New York, USA, pp.
1178 265–292. <https://doi.org/10.1201/9781315154664-12>

1179 Shaheen, S.M., El-Naggar, A., Antoniadis, V., Moghanm, F.S., Zhang, Z., Tsang, D.C.W.,
1180 Ok, Y.S., Rinklebe, J., 2020. Release of toxic elements in fishpond sediments under
1181 dynamic redox conditions: Assessing the potential environmental risk for a safe
1182 management of fisheries systems and degraded waterlogged sediments. J. Environ.
1183 Manage. 255, 109778. <https://doi.org/10.1016/j.jenvman.2019.109778>

1184 Shaheen, S.M., El-Naggar, A., Wang, J., Hassan, N.E.E., Niazi, N.K., Wang, H., Tsang,
1185 D.C.W., Ok, Y.S., Bolan, N., Rinklebe, J., 2018b. Biochar as an (im)mobilizing agent

1186 for the potentially toxic elements in contaminated soils, in: *Biochar from Biomass and*
1187 *Waste*. Elsevier, pp. 255–274. <https://doi.org/10.1016/b978-0-12-811729-3.00014-5>

1188 Shaheen, S.M., Rinklebe, J., Selim, M.H., 2015. Impact of various amendments on
1189 immobilization and phytoavailability of nickel and zinc in a contaminated floodplain
1190 soil. *Int. J. Environ. Sci. Technol.* 12, 2765–2776. [https://doi.org/10.1007/s13762-014-](https://doi.org/10.1007/s13762-014-0713-x)
1191 [0713-x](https://doi.org/10.1007/s13762-014-0713-x)

1192 Shen, Z., Som, A.M., Wang, F., Jin, F., McMillan, O., Al-Tabbaa, A., 2016. Long-term
1193 impact of biochar on the immobilisation of nickel (II) and zinc (II) and the revegetation
1194 of a contaminated site. *Sci. Total Environ.* 542, 771–776.
1195 <https://doi.org/10.1016/j.scitotenv.2015.10.057>

1196 Shen, Z., Zhang, Y., McMillan, O., Jin, F., Al-Tabbaa, A., 2017. Characteristics and
1197 mechanisms of nickel adsorption on biochars produced from wheat straw pellets and
1198 rice husk. *Environ. Sci. Pollut. Res.* 24, 12809–12819. [https://doi.org/10.1007/s11356-](https://doi.org/10.1007/s11356-017-8847-2)
1199 [017-8847-2](https://doi.org/10.1007/s11356-017-8847-2)

1200 Shen, Z., Zhang, Yunhui, Jin, F., Alessi, D.S., Zhang, Yiyun, Wang, F., McMillan, O., Al-
1201 Tabbaa, A., 2018. Comparison of nickel adsorption on biochars produced from mixed
1202 softwood and Miscanthus straw. *Environ. Sci. Pollut. Res.* 25, 14626–14635.
1203 <https://doi.org/10.1007/s11356-018-1674-2>

1204 Shi, Y., Zhang, T., Ren, H., Kruse, A., Cui, R., 2018. Polyethylene imine modified
1205 hydrochar adsorption for chromium (VI) and nickel (II) removal from aqueous solution.
1206 *Bioresour. Technol.* 247, 370–379. <https://doi.org/10.1016/j.biortech.2017.09.107>

1207 Shi, Z., Peltier, E., Sparks, D.L., 2012. Kinetics of Ni sorption in soils: Roles of soil organic
1208 matter and Ni precipitation. *Environ. Sci. Technol.* 46, 2212–2219.
1209 <https://doi.org/10.1021/es202376c>

1210 Shin, W.S., 2017. Adsorption characteristics of phenol and heavy metals on biochar from
1211 *Hizikia fusiformis*. *Environ. Earth Sci.* 76, 782. <https://doi.org/10.1007/s12665-017->

1212 7125-4

1213 Šillerová, H., Chrastný, V., Vítková, M., Francová, A., Jehlička, J., Gutsch, M.R.,
1214 Kocourková, J., Aspholm, P.E., Nilsson, L.O., Berglen, T.F., Jensen, H.K.B., Komárek,
1215 M., 2017. Stable isotope tracing of Ni and Cu pollution in North-East Norway:
1216 Potentials and drawbacks. *Environ. Pollut.* 228, 149–157.
1217 <https://doi.org/10.1016/j.envpol.2017.05.030>

1218 Singh, J., Sharma, M., Basu, S., 2018. Heavy metal ions adsorption and photodegradation of
1219 remazol black XP by iron oxide/silica monoliths: Kinetic and equilibrium modelling.
1220 *Adv. Powder Technol.* 29, 2268–2279. <https://doi.org/10.1016/j.appt.2018.06.011>

1221 Sugawara, E., Nikaido, H., 2014. Properties of AdeABC and AdeIJK efflux systems of
1222 *Acinetobacter baumannii* compared with those of the AcrAB-TolC system of
1223 *Escherichia coli*. *Antimicrob. Agents Chemother.* 58, 7250–7257.
1224 <https://doi.org/10.1128/AAC.03728-14>

1225 Terzano, R., Spagnuolo, M., Vekemans, B., De Nolf, W., Janssens, K., Falkenberg, G., Fiore,
1226 S., Ruggiero, P., 2007. Assessing the origin and fate of Cr, Ni, Cu, Zn, Pb, and V in
1227 industrial polluted soil by combined microspectroscopic techniques and bulk extraction
1228 methods. *Environ. Sci. Technol.* 41, 6762–6769. <https://doi.org/10.1021/es070260h>

1229 Tessier, A., Campbell, P.G.C., Bisson, M., 1979. Sequential extraction procedure for the
1230 speciation of particulate trace metals. *Anal. Chem.* 51, 844–851.
1231 <https://doi.org/10.1021/ac50043a017>

1232 Tongtavee, N., Shiowatana, J., McLaren, R.G., Gray, C.W., 2005. Assessment of lead
1233 availability in contaminated soil using isotope dilution techniques. *Sci. Total Environ.*
1234 348, 244–256. <https://doi.org/10.1016/j.scitotenv.2004.12.066>

1235 Tsadilas, C., Rinklebe, J., 2018. *Nickel in Soils and Plants - 1st Edition*. CRC Press, Taylor
1236 & Francis Group, New York, USA.

1237 Uchimiya, M., Cantrell, K.B., Hunt, P.G., Novak, J.M., Chang, S., 2012. Retention of heavy

1238 metals in a typic kandiudult amended with different manure-based biochars. *J. Environ.*
1239 *Qual.* 41, 1138–1149. <https://doi.org/10.2134/jeq2011.0115>

1240 Uchimiya, M., Chang, S.C., Klasson, K.T., 2011. Screening biochars for heavy metal
1241 retention in soil: Role of oxygen functional groups. *J. Hazard. Mater.* 190, 432–441.
1242 <https://doi.org/10.1016/j.jhazmat.2011.03.063>

1243 Uchimiya, M., Lima, I.M., Thomas Klasson, K., Chang, S., Wartelle, L.H., Rodgers, J.E.,
1244 2010. Immobilization of heavy metal ions (CuII, CdII, NiII, and PbII) by broiler litter-
1245 derived biochars in water and soil. *J. Agric. Food Chem.* 58, 5538–5544.
1246 <https://doi.org/10.1021/jf9044217>

1247 Vasilache, T., Lazar, I., Stamate, M., Nedeff, V., Lazar, G., 2013. Possible environmental
1248 risks of photocatalysis used for water and air depollution - Case of phosgene generation.
1249 *APCBEE Procedia* 5, 181–185. <https://doi.org/10.1016/j.apcbee.2013.05.032>

1250 Venegas, A., Rigol, A., Vidal, M., 2016. Effect of ageing on the availability of heavy metals
1251 in soils amended with compost and biochar: evaluation of changes in soil and
1252 amendment properties. *Environ. Sci. Pollut. Res.* 23, 20619–20627.
1253 <https://doi.org/10.1007/s11356-016-7250-8>

1254 Vilvanathan, S., Shanthakumar, S., 2017. Continuous biosorption of nickel from aqueous
1255 solution using chrysanthemum indicum derived biochar in a fixed-bed column. *Water*
1256 *Sci. Technol.* 76, 1895–1906. <https://doi.org/10.2166/wst.2017.289>

1257 Wang, He, Wang, Han, Zhao, H., Yan, Q., 2020. Adsorption and Fenton-like removal of
1258 chelated nickel from Zn-Ni alloy electroplating wastewater using activated biochar
1259 composite derived from Taihu blue algae. *Chem. Eng. J.* 379, 122372.
1260 <https://doi.org/10.1016/j.cej.2019.122372>

1261 Wang, T., Liu, Y., Wang, J., Wang, X., Liu, B., Wang, Y., 2019. In-situ remediation of
1262 hexavalent chromium contaminated groundwater and saturated soil using stabilized
1263 iron sulfide nanoparticles. *J. Environ. Manage.* 231, 679–686.

1264 <https://doi.org/10.1016/j.jenvman.2018.10.085>

1265 WHO, 2000. Chapter 6.10 Nickel General description [WWW Document]. Air Qual. Guidel.
1266 - Second Ed. URL
1267 [https://www.euro.who.int/__data/assets/pdf_file/0014/123080/AQG2ndEd_6_10Nickel](https://www.euro.who.int/__data/assets/pdf_file/0014/123080/AQG2ndEd_6_10Nickel.pdf)
1268 .pdf (accessed 4.5.21).

1269 WHO, 1996. Permissible limits of heavy metals in soil and plants, Geneva, Switzerland.

1270 Wu, H., Tan, H.L., Toe, C.Y., Scott, J., Wang, L., Amal, R., Ng, Y.H., 2020. Photocatalytic
1271 and photoelectrochemical systems: Similarities and differences. Adv. Mater. 32:18,
1272 1904717. <https://doi.org/10.1002/adma.201904717>

1273 Wu, H., Zheng, Z., Tang, Y., Huang, N.M., Amal, R., Lim, H.N., Ng, Y.H., 2018. Pulsed
1274 electrodeposition of CdS on ZnO nanorods for highly sensitive photoelectrochemical
1275 sensing of copper (II) ions. Sustain. Mater. Technol. 18, e00075.
1276 <https://doi.org/10.1016/j.susmat.2018.e00075>

1277 Wurzer, C., Masek, O., Sohi, S., Mašek, O., 2020. Synergies in sequential biochar systems,
1278 in: Green Carbon. ETN, pp. 147–159.

1279 Xue, Y., Gao, B., Yao, Y., Inyang, M., Zhang, M., Zimmerman, A.R., Ro, K.S., 2012.
1280 Hydrogen peroxide modification enhances the ability of biochar (hydrochar) produced
1281 from hydrothermal carbonization of peanut hull to remove aqueous heavy metals:
1282 Batch and column tests. Chem. Eng. J. 200, 673–680.
1283 <https://doi.org/10.1016/j.cej.2012.06.116>

1284 Yang, L., He, L., Xue, J., Wu, L., Ma, Y., Li, H., Peng, P., Li, M., Zhang, Z., 2019. Highly
1285 efficient nickel (II) removal by sewage sludge biochar supported α -Fe₂O₃ and α -
1286 FeOOH: Sorption characteristics and mechanisms. PLoS One 14, e0218114.
1287 <https://doi.org/10.1371/journal.pone.0218114>

1288 Yang, X., Tsibart, A., Nam, H., Hur, J., El-Naggar, A., Tack, F.M.G., Wang, C.-H., Lee,
1289 Y.H., Tsang, D.C.W., Ok, Y.S., 2019. Effect of gasification biochar application on soil

1290 quality: Trace metal behavior, microbial community, and soil dissolved organic matter.
1291 *J. Hazard. Mater.* 365, 684–694. <https://doi.org/10.1016/j.jhazmat.2018.11.042>

1292 Yuan, Y., Bolan, N., PrévotEAU, A., Vithanage, M., Biswas, J.K., Wang, H., 2017.
1293 Applications of biochar in redox-mediated reactions. *Bioresour. Technol.* 246, 271–281.
1294 <https://doi.org/10.1016/J.BIORTECH.2017.06.154>

1295 Zama, E.F., Reid, B.J., Arp, H.P.H., Sun, G.X., Yuan, H.Y., Zhu, Y.G., 2018. Advances in
1296 research on the use of biochar in soil for remediation: a review. *J. Soils Sediments* 18,
1297 2433–2450. <https://doi.org/10.1007/s11368-018-2000-9>

1298 Zambelli, B., Uversky, V.N., Ciurli, S., 2016. Nickel impact on human health: An intrinsic
1299 disorder perspective. *Biochim. Biophys. Acta - Proteins Proteomics.* 1864, 1714–1731.
1300 <https://doi.org/10.1016/j.bbapap.2016.09.008>

1301 Zelano, I.O., Sivry, Y., Quantin, C., Gelabert, A., Maury, A., Phalyvong, K., Benedetti, M.F.,
1302 2016. An isotopic exchange kinetic model to assess the speciation of metal available
1303 pool in soil: The case of nickel. *Environ. Sci. Technol.* 50, 12848–12856.
1304 <https://doi.org/10.1021/acs.est.6b02578>

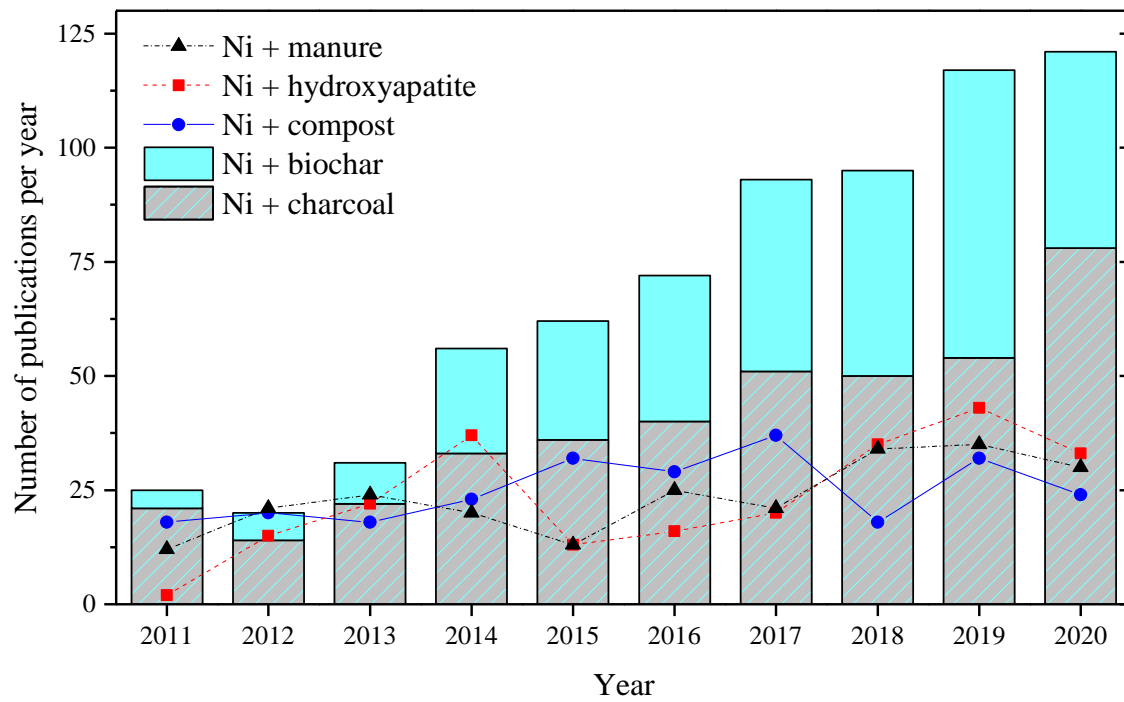
1305 Zhang, A., Li, X., Xing, J., Xu, G., 2020. Adsorption of potentially toxic elements in water
1306 by modified biochar: A review. *J. Environ. Chem. Eng.* 8, 104196.
1307 <https://doi.org/10.1016/j.jece.2020.104196>

1308 Zhu, L., Tong, L., Zhao, N., Li, J., Lv, Y., 2019. Coupling interaction between porous
1309 biochar and nano zero valent iron/nano A-hydroxyl iron oxide improves the
1310 remediation efficiency of cadmium in aqueous solution. *Chemosphere* 219, 493–503.
1311 <https://doi.org/10.1016/j.chemosphere.2018.12.013>

1312 Zou, Q., Xiang, H., Jiang, J., Li, D., Aihemaiti, A., Yan, F., Liu, N., 2019. Vanadium and
1313 chromium-contaminated soil remediation using VFAs derived from food waste as soil
1314 washing agents: A case study. *J. Environ. Manage.* 232, 895–901.
1315 <https://doi.org/10.1016/j.jenvman.2018.11.129>

1316

1317

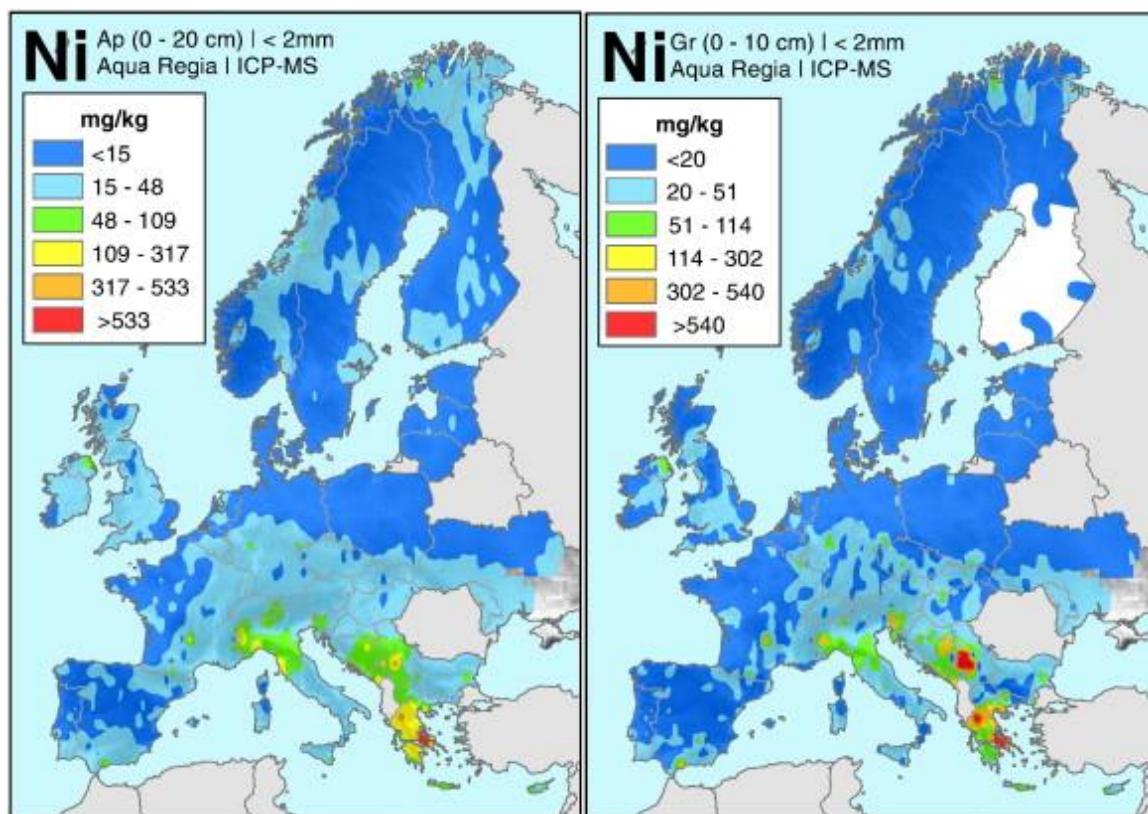


1318

1319 Figure 1: The number of publications in the SCOPUS database based on the following
 1320 keywords: biochar and nickel, charcoal and nickel, compost and nickel, manure and nickel,
 1321 and hydroxyapatite and nickel.

1322

1323



1324

1325

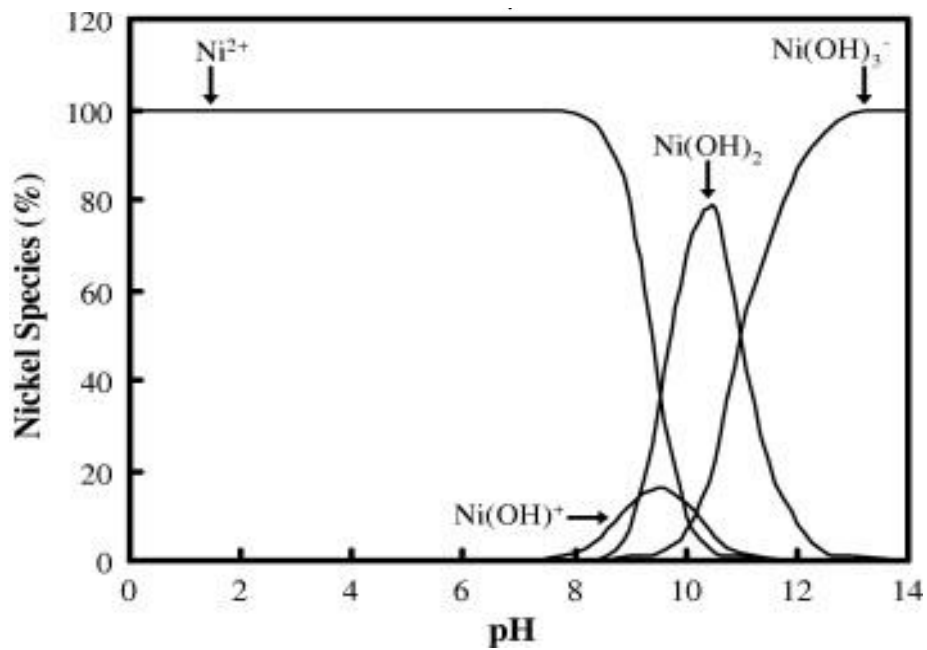
1326 Figure 2: Maps of Ni concentrations in soils collected from agricultural (Ap) and grazing

1327 land (Gr) in Europe determined by ICP-MS following an aqua regia extraction. (reproduced

1328 from Albanese et al. (2015), with permission from the publisher)

1329

1330



1331

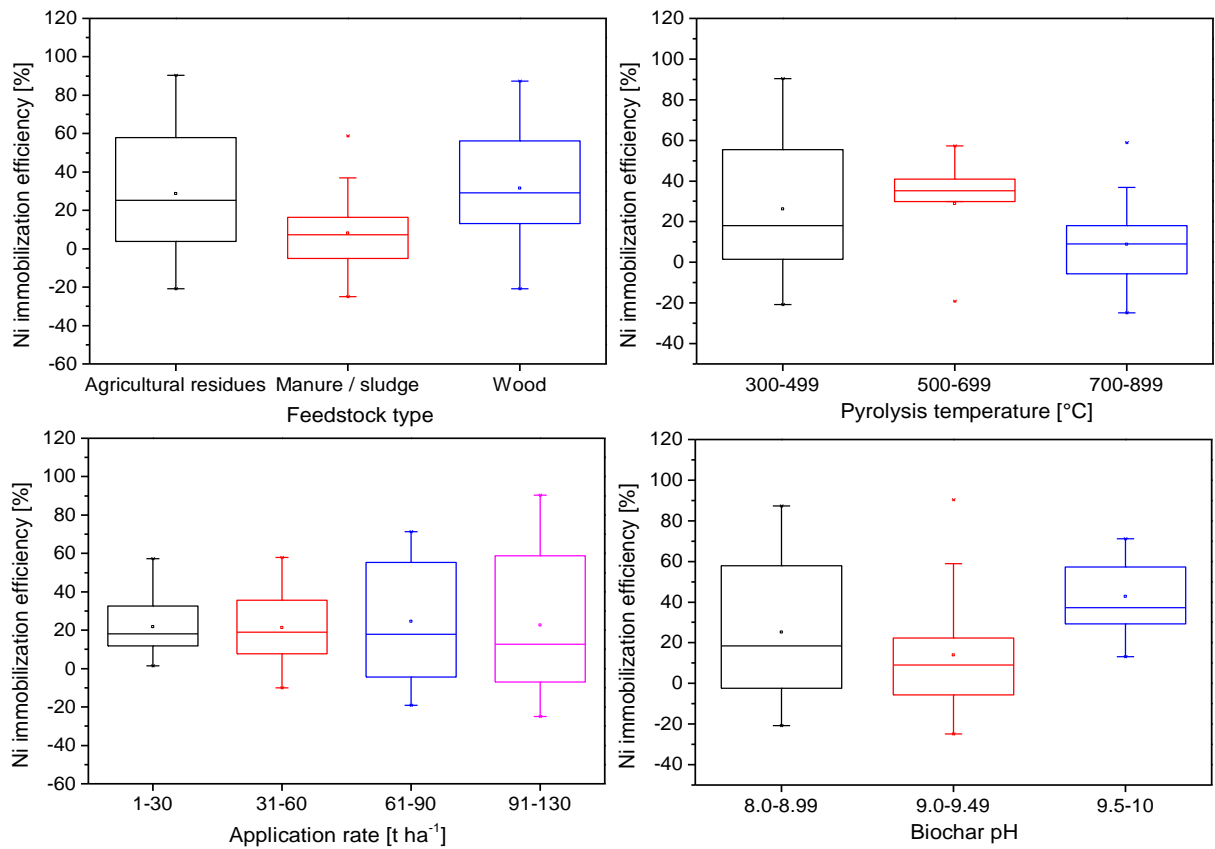
1332

1333 Figure 3: The speciation of Ni in aqueous solutions in the absence of oxidizing agents

1334 (Adapted from Anoop Krishnan et al. (2011), with permission from the publisher)

1335

1336



1337
1338

1339 Figure 4: The nickel immobilization efficiency of biochars as affected by biochar properties.

1340 Data are extracted from eight studies (based on a total of 59 individual observations). The
 1341 box chart is represented by the median (centerline), mean (dot), lower and upper quartiles
 1342 (the lower and upper borders of the box, respectively), whiskers-error bars (the minimum
 1343 and maximum observations) (Bogusz and Oleszczuk, 2018; Eissa, 2019; Ibrahim et al., 2019;
 1344 Munir et al., 2020; Nawab et al., 2018; Rehman et al., 2016; Rodríguez-Vila et al., 2015;
 1345 Venegas et al., 2016)

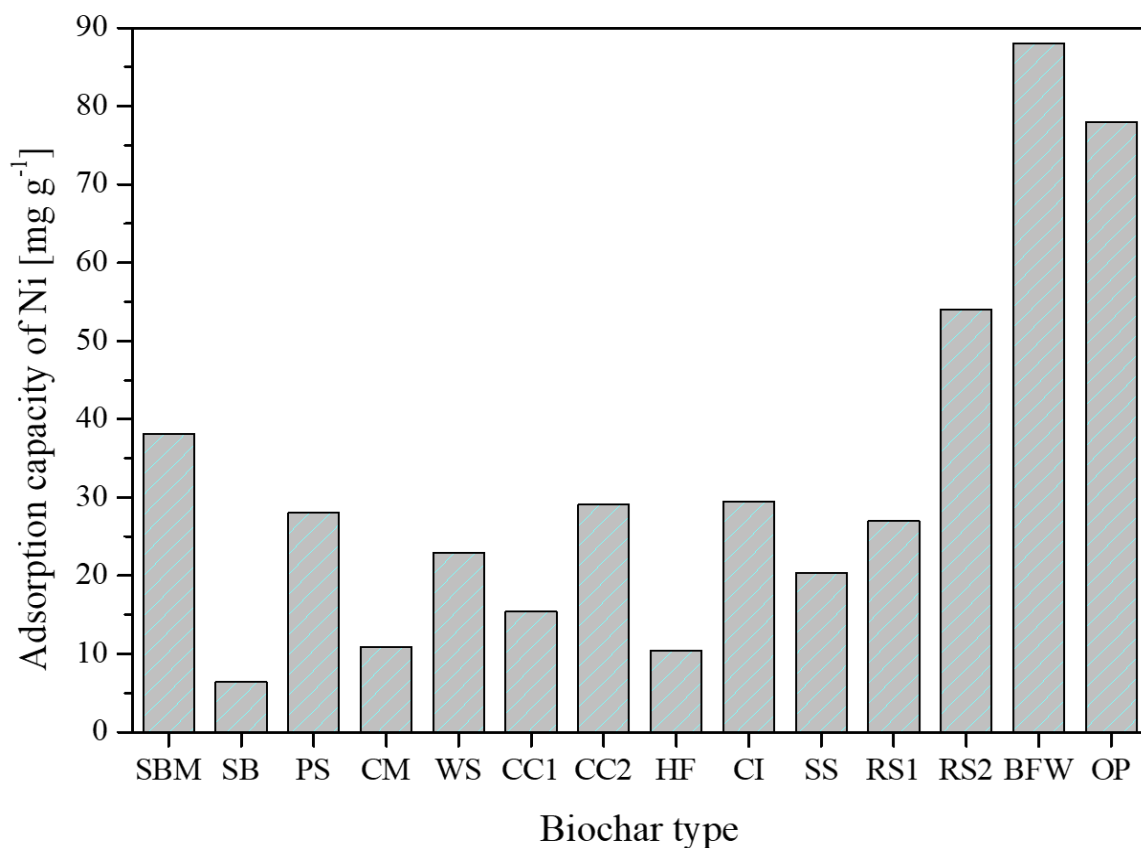
1346

1347

1348

1349

1350



1351

1352

1353 Figure 5: Adsorption capacity of Ni on biochar produced from different feedstocks. Data are
 1354 obtained from different studies as follows (abbreviation: type of biochar feedstock with
 1355 references cited): SBM: Sugarcane bagasse (milled) (Lyu et al., 2018), SB: Sugarcane
 1356 bagasse (un-milled) (Lyu et al., 2018), PS: Palm seed (Gazi et al., 2018), CM: chicken
 1357 manure (Higashikawa et al., 2016), WS: wheat straw pellets (Shen et al., 2017), CC1:
 1358 corncobs (Hu et al., 2018), CC2: corncobs (Shi et al., 2018), HF: hizikia fusiformis (Shin,
 1359 2017), CI: chrysanthemum indicum (Vilvanathan and Shanthakumar, 2017), SS: sewage
 1360 sludge (Yang et al., 2019), RS1: rice straw (Deng et al., 2019), RS2: rice straw (Deng et al.,
 1361 2019), BFW: banana fruit waste, and OP: orange peel (Amin et al., 2019)

1362

1363

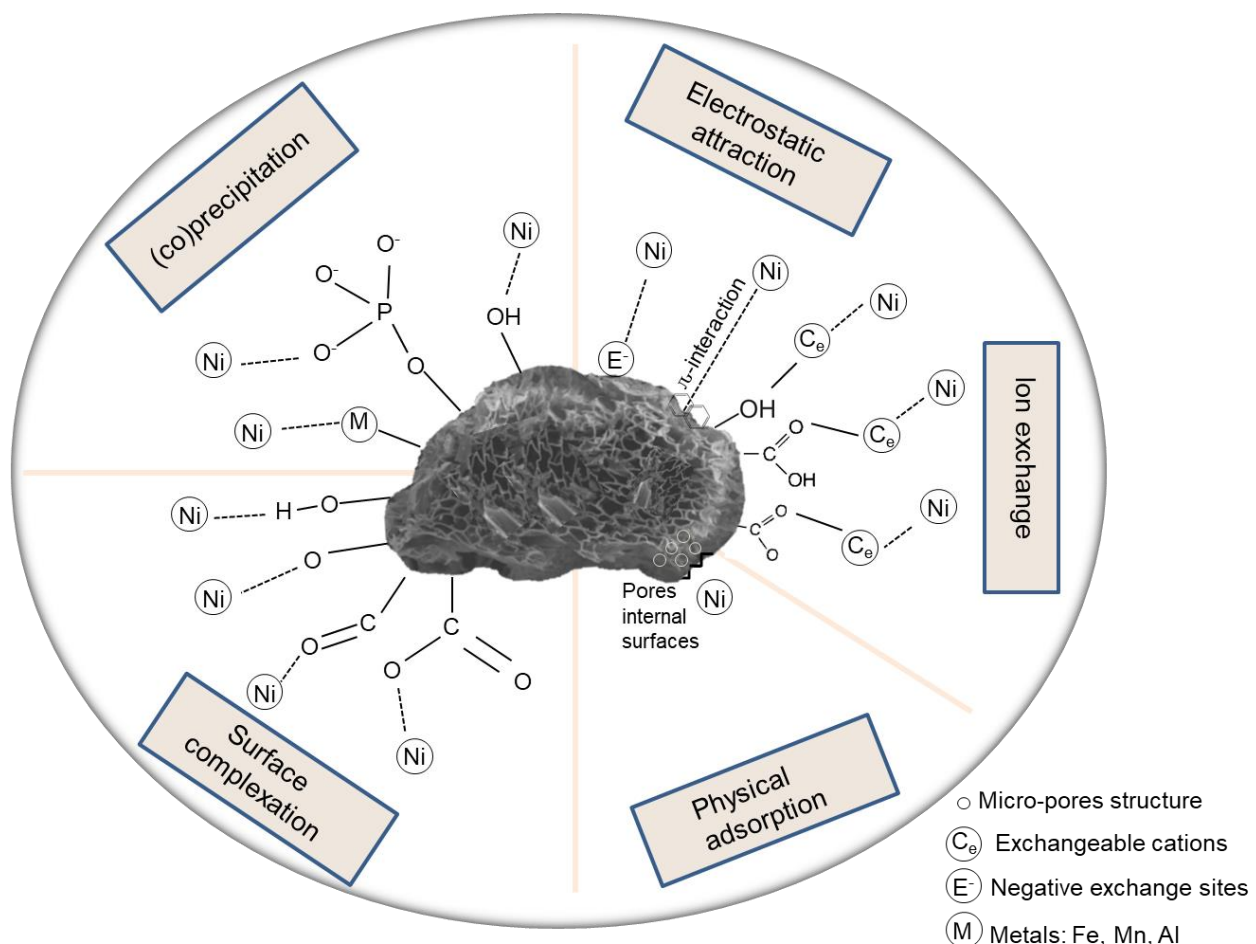


Figure 6: A schematic diagram of mechanisms of interactions between biochar and Ni

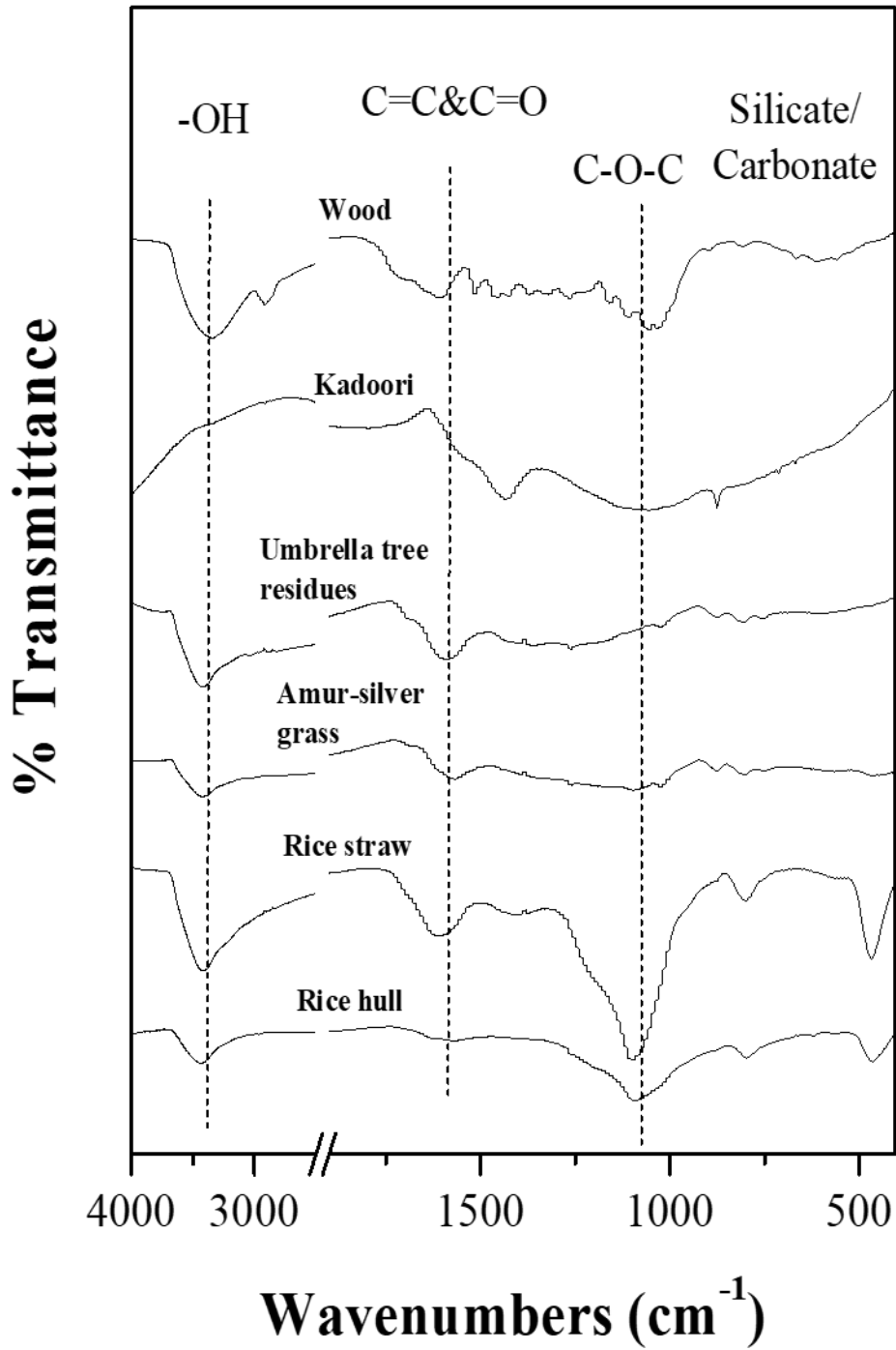


Figure 7: Fourier-transform infrared spectra of six types of biochars produced from different feedstocks. Data are obtained from previous studies (El-Naggar et al., 2018a; Rinklebe et al., 2020)

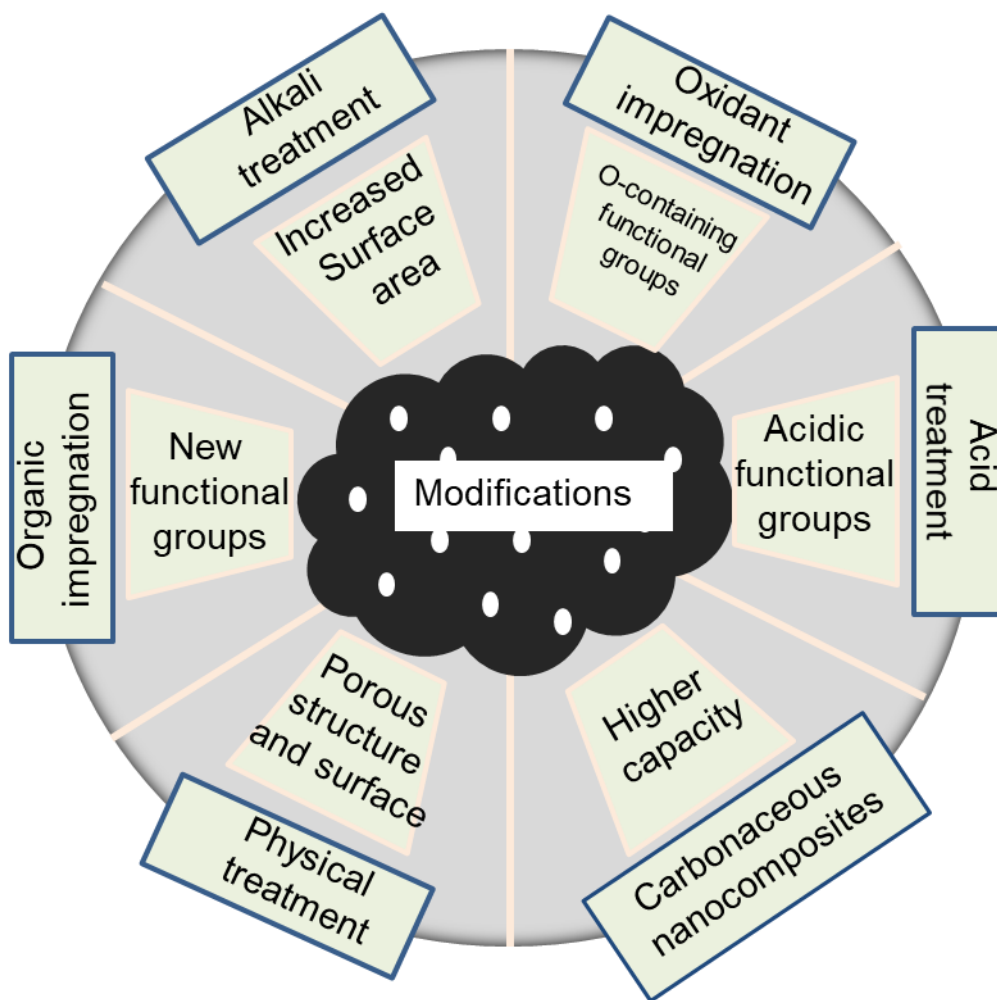


Figure 8: A schematic diagram illustrating recently proposed methods of biochar modification for the remediation of Ni contamination

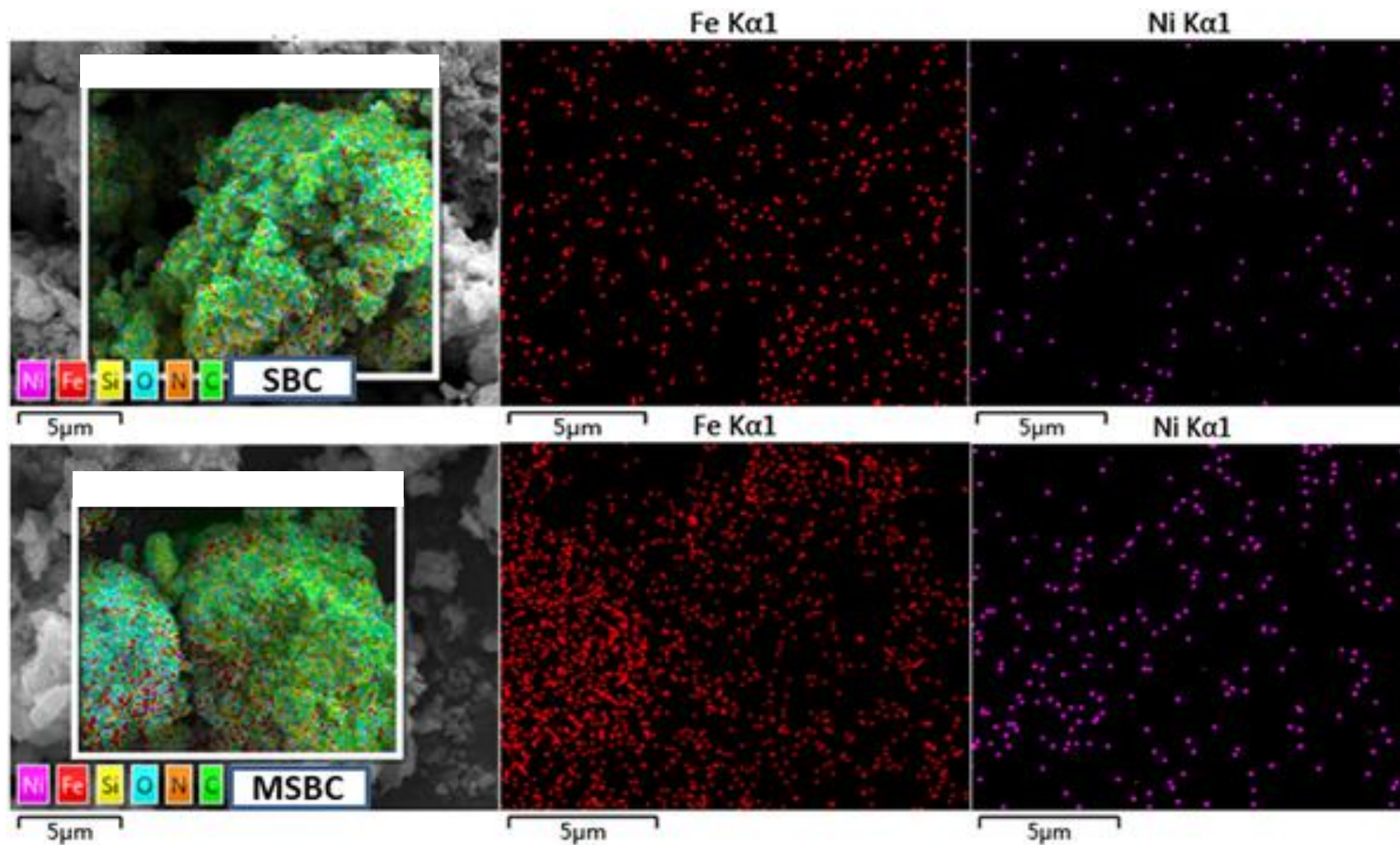


Figure 10: Scanning electron microscopy with energy dispersive x-ray analysis on the surface of sewage sludge biochar (SBC), sewage sludge biochar supported α -Fe₂O₃ and α -FeOOH (MSBC) after Ni adsorption (reproduced from Yang et al. (2019), with permission from the publisher)